



HAL
open science

Roadmap for daily practice of CBCT in cleft lip palate paediatric patients: a pictorial review

Raphael Olszewski, Antoine de Muylder, Sergio Siciliano

► To cite this version:

Raphael Olszewski, Antoine de Muylder, Sergio Siciliano. Roadmap for daily practice of CBCT in cleft lip palate paediatric patients: a pictorial review. *NEMESIS Negative effects in medical science: oral and maxillofacial surgery*, 2023, 30 (1), pp.1-50. 10.14428/nemesis.v30i1 . hal-04216191

HAL Id: hal-04216191

<https://hal.science/hal-04216191v1>

Submitted on 23 Sep 2023

HAL is a multi-disciplinary open access archive for the deposit and dissemination of scientific research documents, whether they are published or not. The documents may come from teaching and research institutions in France or abroad, or from public or private research centers.

L'archive ouverte pluridisciplinaire **HAL**, est destinée au dépôt et à la diffusion de documents scientifiques de niveau recherche, publiés ou non, émanant des établissements d'enseignement et de recherche français ou étrangers, des laboratoires publics ou privés.



Distributed under a Creative Commons Attribution - ShareAlike 4.0 International License



1
2
3
4
5
6
7
8

9

10
11
12
13
14
15
16
17
18
19
20
21
22

Roadmap for daily practice of CBCT in cleft lip palate paediatric patients: a pictorial review.

Authors:
Olszewski R DDS, MD, PhD, DrSc, Prof^{1,2*},
De Muylder A MD, DDS¹,
Siciliano S MD, DDS³

Affiliations:

¹ Department of oral and maxillofacial surgery, Cliniques universitaires Saint Luc, UCLouvain, Brussels, Belgium
² Oral and maxillofacial surgery research Lab (OMFS Lab), NMSK, IREC, UCLouvain, Brussels, Belgium
³ Department of oral and maxillofacial surgery, Clinique Sainte Elisabeth, Brussels, Belgium
*Corresponding author: Prof Raphael Olszewski, Department of oral and maxillofacial surgery, Cliniques universitaires Saint Luc, UCLouvain, Av. Hippocrate 10, 1200 Brussels, Belgium, email: Raphael.olszewski@saintluc.uclouvain.be ORCID ID: orcid.org/0000-0002-2211-7731

Disclaimer: the views expressed in the submitted article are our own and not an official position of the institution or funder.

23

24

Abstract

25

Objective: to present and to illustrate a new methodology for daily practice in cone beam computed tomography (CBCT) interpretation and reporting in cleft lip palate (CLP) non syndromic paediatric patients. The proposed protocol is based on clinical experience and on systematic search of the literature.

26

27

28

29

30

Material and methods: We performed two types of systematic search of articles: 1) articles related to the use of CBCT in CLP patients, and 2) articles related to the reporting and interpretation of the CBCT images by radiologists. We used two databases PubMed and Google scholar.

31

32

33

34

35

Results: For indications of CBCT in CLP patients we found in PubMed 378 articles and 48 articles were selected for the review; in Google scholar we found 463 articles, and 9 articles were selected for the review. 2) For reporting in CBCT we found 956 articles in PubMed, and 9 articles were selected for the review.

36

37

38

39

40

Conclusions: We presented the 6-steps system for interpretation and reporting information from CBCT of CLP paediatric patients: 1) Step 1 (axial view): presence or absence of bone bridge remnants of alveolar bone graft; Step 2 (3D dental tissue reconstruction): description of dental arch tooth by tooth, search for agenesis and supernumerary teeth, description of variation in the position of the tooth explaining the type of existing translation and rotation; Step 3 (coronal view): cleft palate pathway and its extension; anomaly in maxillary, ethmoid and sphenoid sinuses if existing; Step 4 (sagittal and coronal view): checking of the opening (calcification sites) of the sphenoccipital synchondrosis, and checking of anomalies of the occipital bone; Step 5 (3D bone tissue reconstruction): C1-C2 vertebra anomalies; Step 6 (3D soft tissue reconstruction): external ear anomalies. We illustrated our methodology with 46 figures from 5 CBCT of CLP patients.

41

42

43

44

45

46

47

48

49

50

51

52

Keywords: cone beam computed tomography, CBCT, cleft lip palate, paediatric, reporting

53

54

55

56

57

Introduction

58

59

60

61

62

63

64

65

66

67

68

69

70

71

72

73

74

75

76

77

78

79

80

81

82

83

84

85

86

87

88

89

90

91

92

93

94

95

96

97

The main indication of using cone beam computed tomography (CBCT) in paediatric dentistry is related to cleft palate and cleft lip palate (CLP) patients [1, 2]. The CBCT was mainly used in CLP patients to study the secondary alveolar bone grafting [3- 29]. CBCT was also used to evaluate maxillary expansion in CLP patients [6, 30-36]. Moreover, CBCT was also used in various anatomical studies related with CLP patients: 1) Three-dimensional (3D) analysis of craniofacial structures [3, 29, 37], and of facial asymmetry [29, 38, 39]; 2) mandible [3, 29, 40, 41]; 3) sella turcica [42]; 4) pharyngeal airway volume [3, 43-48]; 5) cortical bone thickness around the cleft area [26, 27, 29, 49]; 6) palatal morphology and soft tissue depth [6, 28, 29, 50, 51]; 7) maxillary sinus volume [29, 52, 53]; 8) nasal morphology [3, 29, 54], and nasal airway [55]; 9) canine eruption through the alveolar graft bone [3, 4, 6, 7, 27, 56, 57]; 10) quantity, and morphological variation of teeth present around the cleft [3, 5-7, 27, 29, 57]; 11) cervical vertebrae [58]. However, all of these studies do not give guidance in reporting information from CLP CBCT examinations.

Limited guidelines for reporting CBCT dataset were already proposed in endodontics [59-61], implantology [59, 60], periodontology [60], lower third molars [60], and in orthodontics [60, 62]. There exists an agreement between authors that all the field of view must be viewed and described when reporting CBCT images [57, 59, 60, 63, 64].

However, Miles et al. reported that 98% of medical radiology residents received no formal training in radiology reporting [64], and 78% learned the process from a fellow resident [64]. Therefore, Miles et al. proposed to introduce a new software (Easyriter) for building structured CBCT reports including: 1) Paranasal sinuses, 2) Nasal cavity, 3) Airway, 4) Cervical structures, 5) Temporomandibular joints (TMJ), 6) Dental findings, and 7) Other findings [64]. Kachlan et al., described structured CBCT reports for incidental findings in craniomaxillofacial and cervical area: 1) Jaws, 2) Paranasal sinus, 3) Nasal fossa, 4) Pharyngeal airway, 5) TMJ, 6) Skull base/brain, 7) Neck soft tissues, and 8) Others [65].

Only two articles were related to the reporting of CBCT findings in CLP patients [66, 67].

Santos et al. described incidental findings in CLP patients situated in the following areas: 1) Skull, 2) Paranasal sinuses, 3) Orbit, 4) Middle and inner ear cavity, 5) Pharynx, 6) TMJ, 7) Cervical spine, 8) Maxilla, and 9) Mandible [66]. Only general information was given by the authors on CBCT image modalities used to search for incidental findings such as 3D reconstructions with varying opacities, reconstructed panoramic radiographs, and axial slices of the maxilla and mandible [66].

The authors also found anomalies in dental development including supernumerary teeth, teeth with atypical crown and/or root morphology, missing, ectopic, and impacted dentition [66]. The article by Santos et al is accessible in closed access

98 only (paywall). The article contains only 4 figures: one axial slice without any
99 anomaly, and three 3D reconstruction figures without arrows showing 1) an ectopic
100 impacted central incisor, 2) a missing lateral maxillary incisor, and 3) impacted
101 maxillary canine.
102 Bezerra et al., [67] separated dental development anomalies in CLP patients into 3
103 categories: 1) Agenesis (second incisor, second premolar), 2) Microdontia (conical
104 lateral incisor), and 3) Giroversion (central incisor). The article by Bezerra et al is
105 accessible in open access (free article for readers) [67]. However, three figures show
106 only the presence of left alveolar cleft [67]. Figures that may illustrate dental
107 development anomalies are missing [67].
108 The aim for our article was to present and to illustrate a new methodology for daily
109 practice in CBCT interpretation and reporting in CLP non syndromic paediatric
110 patients. The proposed protocol is based on clinical experience and on systematic
111 search of the literature.

112 **Materials and methods**

113 We performed two types of systematic search of articles for this review: 1) articles
114 related to the use of CBCT in CLP patients, and 2) articles related to the reporting
115 and interpretation of the CBCT images by radiologists.
116

117 **1. Search for articles related to the use of CBCT in CLP** 118 **patient**

119 First, we systematically searched for articles related to the use of CBCT in CLP
120 patients in PubMed and in Google Scholar. The inclusion criteria were: patients with
121 maximal age of 13 years-old, and studies centred on the use of CBCT. The exclusion
122 criteria were: CLP in adult patients, mixed groups with included children below and
123 over 13-years-old, experimental studies, animal studies, studies where the age of
124 patients was not given, and articles without abstract. The criterium of the threshold
125 of the patient age is related to the fact that the late alveolar surgery in CLP patients
126 is performed until the age of 13 years-old. We selected articles only in English
127 without a limit of time. One observer performed the search. The articles were
128 selected based on the title and abstract.

129 In PubMed we used the following search equations:

130
131 1. PubMed "cbct"[All Fields] AND ("cleft"[All Fields] OR "clefted"[All Fields] OR
132 "clefting"[All Fields] OR "clefts"[All Fields]). The search was performed on
133 30.12.2022. We found 206 articles, and 47 articles were selected for final review [3,
134 6-25, 30-50, 52-56].

135
136 2. PubMed "cbct"[All Fields] AND ("cleft"[All Fields] OR "clefted"[All Fields] OR
137 "clefting"[All Fields] OR "clefts"[All Fields]) AND ("applicabilities"[All Fields]

138 OR "applicability"[All Fields] OR "application"[All Fields] OR "applications"[All
139 Fields] OR "applicative"[All Fields]). The search was performed on 30.12.2022. We
140 found 20 articles, and 1 article was selected for final review [1].

141

142 3. PubMed "cbct"[All Fields] AND ("cleft"[All Fields] OR "clefted"[All Fields] OR
143 "clefting"[All Fields] OR "clefts"[All Fields]) AND ("evaluability"[All Fields] OR
144 "evaluate"[All Fields] OR "evaluated"[All Fields] OR "evaluates"[All Fields] OR
145 "evaluating"[All Fields] OR "evaluation"[All Fields] OR "evaluation s"[All Fields]
146 OR "evaluations"[All Fields] OR "evaluative"[All Fields] OR "evaluatively"[All
147 Fields] OR "evaluatives"[All Fields] OR "evaluator"[All Fields] OR "evaluator
148 s"[All Fields] OR "evaluators"[All Fields]). The search was performed on
149 30.12.2022. We found 132 articles, and no articles were selected.

150

151 4. PubMed "cbct"[All Fields] AND ("protocol"[All Fields] OR "protocol s"[All
152 Fields] OR "protocolized"[All Fields] OR "protocols"[All Fields]) AND ("cleft"[All
153 Fields] OR "clefted"[All Fields] OR "clefting"[All Fields] OR "clefts"[All Fields]).
154 The search was performed on 30.12.2022. We found 20 articles, and no articles were
155 selected.

156

157 In Pubmed we found 378 articles and 48 articles were finally selected for the review
158 [1, 3, 6-25, 30-50, 52-56].

159 In Google Scholar we used the following search equation: "children with cleft lip
160 and palate CBCT 3D". The search was performed on 30.12.2022. We found 463
161 articles, and 9 articles were finally selected after full text lecture [2, 4, 5, 26-28, 51,
162 57, 58].

163

164 **2. Search for articles related to the reporting and interpretation of the images by radiologists**

165

166 We used only PubMed database. The selected articles were only in English. The
167 inclusion criteria were the articles with abstract, the articles related to the reporting
168 CBCT examinations in dentistry (including orthodontics) and in maxillofacial sur-
169 gery.

169

170 In PubMed we used the 4 following search equations:

171

172 1. PubMed: "interpretation CBCT"
173 ("interpret"[All Fields] OR "interpretability"[All Fields] OR "interpretable"[All
174 Fields] OR "interpretating"[All Fields] OR "interpretation"[All Fields] OR "interpre-
175 tation s"[All Fields] OR "interpretational"[All Fields] OR "interpretations"[All
176 Fields] OR "interpretative"[All Fields] OR "interpreted"[All Fields] OR
177 "interpreter"[All Fields] OR "interpreter s"[All Fields] OR "interpreters"[All Fields]
178 OR "interpreting"[All Fields] OR "interpretive"[All Fields] OR "interpretively"[All
Fields] OR "interprets"[All Fields]) AND "CBCT"[All Fields]

179 **Translations interpretation:** "interpret"[All Fields] OR "interpretability"[All
 180 Fields] OR "interpretable"[All Fields] OR "interpretating"[All Fields] OR
 181 "interpretation"[All Fields] OR "interpretation's"[All Fields] OR
 182 "interpretational"[All Fields] OR "interpretations"[All Fields] OR "interpreta-
 183 tive"[All Fields] OR "interpreted"[All Fields] OR "interpreter"[All Fields] OR
 184 "interpreter's"[All Fields] OR "interpreters"[All Fields] OR "interpreting"[All
 185 Fields] OR "interpretive"[All Fields] OR "interpretively"[All Fields] OR
 186 "interprets"[All Fields]

187 We performed this search on 26.11.2022. We found 755 articles, and 6 articles were
 188 selected after full lecture of articles [59, 60, 62-65].
 189

190 2. PubMed: "CBCT reporting guidelines"
 191 "CBCT"[All Fields] AND ("reportable"[All Fields] OR "reporting"[All Fields] OR
 192 "reportings"[All Fields] OR "research report"[MeSH Terms] OR ("research"[All
 193 Fields] AND "report"[All Fields]) OR "research report"[All Fields] OR "report"[All
 194 Fields] OR "reported"[All Fields] OR "reports"[All Fields]) AND
 195 ("guideline"[Publication Type] OR "guidelines as topic"[MeSH Terms] OR
 196 "guidelines"[All Fields])

197 We performed this search on 29.12.2022. We found 58 articles, and 1 article was
 198 selected [61].
 199

200 3. PubMed: "reporting interpretation CBCT"
 201 ("reportable"[All Fields] OR "reporting"[All Fields] OR "reportings"[All Fields] OR
 202 "research report"[MeSH Terms] OR ("research"[All Fields] AND "report"[All
 203 Fields]) OR "research report"[All Fields] OR "report"[All Fields] OR "reported"[All
 204 Fields] OR "reports"[All Fields]) AND ("interpret"[All Fields] OR
 205 "interpretability"[All Fields] OR "interpretable"[All Fields] OR "interpretating"[All
 206 Fields] OR "interpretation"[All Fields] OR "interpretation s"[All Fields] OR
 207 "interpretational"[All Fields] OR "interpretations"[All Fields] OR
 208 "interpretative"[All Fields] OR "interpreted"[All Fields] OR "interpreter"[All Fields]
 209 OR "interpreter s"[All Fields] OR "interpreters"[All Fields] OR "interpreting"[All
 210 Fields] OR "interpretive"[All Fields] OR "interpretively"[All Fields] OR
 211 "interprets"[All Fields]) AND "CBCT"[All Fields]

212 We performed this search on 26/11/2022. We found 109 articles, and no articles
 213 were finally selected.
 214

215 4. PubMed: "CBCT cleft reporting"
 216 "CBCT"[All Fields] AND ("cleft"[All Fields] OR "clefted"[All Fields] OR
 217 "clefting"[All Fields] OR "clefts"[All Fields]) AND ("reportable"[All Fields] OR
 218 "reporting"[All Fields] OR "reportings"[All Fields] OR "research report"[MeSH
 219 Terms] OR ("research"[All Fields] AND "report"[All Fields]) OR "research
 220 report"[All Fields] OR "report"[All Fields] OR "reported"[All Fields] OR
 221 "reports"[All Fields])

222 **Translations cleft:** "cleft"[All Fields] OR "clefted"[All Fields] OR "clefting"[All
 223 Fields] OR "clefts"[All Fields]

224 **Translations reporting:** "reportable"[All Fields] OR "reporting"[All Fields] OR
225 "reportings"[All Fields] OR "research report"[MeSH Terms] OR ("research"[All
226 Fields] AND "report"[All Fields]) OR "research report"[All Fields] OR "report"[All
227 Fields] OR "reported"[All Fields] OR "reports"[All Fields]

228 We performed this search on 21.12.2022. We found 34 articles, and 2 articles were
229 finally selected after full lecture [66, 67].

230

231 Finally, 956 articles were found, and 9 articles were selected for the review on the
232 reporting and interpretation of dentomaxillofacial CBCT [59, 60, 62-67].

233 The selected articles on CBCT applications in CLP were used in introduction
234 section. The selected articles on interpretation and reporting CBCT information
235 were used in introduction, results and in discussion section.

236

237

Results

238 There were 6 closed access (paywall) [59, 61, 62, 64-66], and 3 open access (free
239 for reading) articles [60, 63, 67] among the 9 articles selected on reporting and
240 interpretation of dentomaxillofacial CBCT.

241 Seven articles provided no figures on cleft palate in CBCT [59-65]. Only two
242 articles contained some figures of CBCT CLP patients [66, 67]. One article was
243 available in closed access [66] and contained 4 figures: one axial view without cleft,
244 3 figures with 3D reconstruction showing 1) ectopic central incisor, 2) missing
245 maxillary lateral incisor, 3) impacted maxillary canine. Only one article was
246 accessible free of charge (open access) [67] and contained three figures of left CLP
247 (one axial view and two 3D reconstructions without arrows).

248 We used Planmeca Promax 3D mid CBCT with 90Kvp generator. The radiological
249 protocol was set as following: 200µm slice thickness, 16x6.2cm (diameter x height)
250 field of view including maxilla, skull base, C1 and C2 vertebra. We used an ultra-
251 low dose protocol for all our patients as they were children. The acquisition time
252 was of 6 seconds.

253 We used the following 6-steps system for interpretation and reporting information
254 from CBCT of CLP paediatric patients:

255 Step 1. Axial view: we searched for presence or absence of bone bridge remnants of
256 alveolar bone graft (iliac crest).

257 Step 2. 3D dental tissue reconstruction: we describe dental arch from tooth n°18/17
258 to n°28/27, we search for agenesis and supernumerary teeth, we describe each
259 variation in the position of the tooth explaining the type of existing translation and
260 rotation.

261 Step 3. Coronal view: we search for cleft palate pathway and its extension; we
262 describe any anomaly in maxillary, ethmoid and sphenoid sinuses if existing.

263 Step 4. Sagittal and coronal view: we check the opening (calcification sites) of the
264 sphenoccipital synchondrosis, and we are checking potential anomalies of the
265 occipital bone.

266 Step 5. 3D bone tissue reconstruction: we search for C1-C2 vertebra anomalies.
267 Step 6. 3D soft tissue reconstruction: we search for external ear anomalies. In
268 Planmeca Promax 3D mid CBCT only the right external ear is almost accessible for
269 interpretation. The left external ear is cut at the level of the left external auditory
270 canal.
271 We illustrate our 6-steps system for interpretation and reporting CBCT information
272 in the 5 following clinical examples.
273

274 **1. Patient 9 years-old, left cleft lip palate, 3 weeks**
275 **postoperative control**

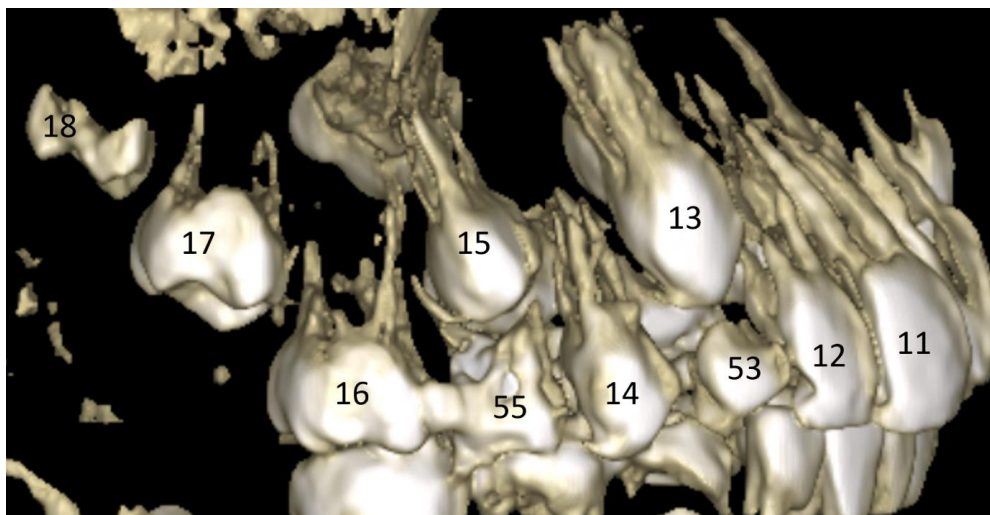
276 Step 1. Axial view: we search for presence or absence of bone bridge remnants of
277 alveolar bone graft (iliac crest).



278
279 **Fig. 1. Axial view.** Arrows: presence of bone bridge of alveolar bone graft
280 between teeth n°21 and n°23.

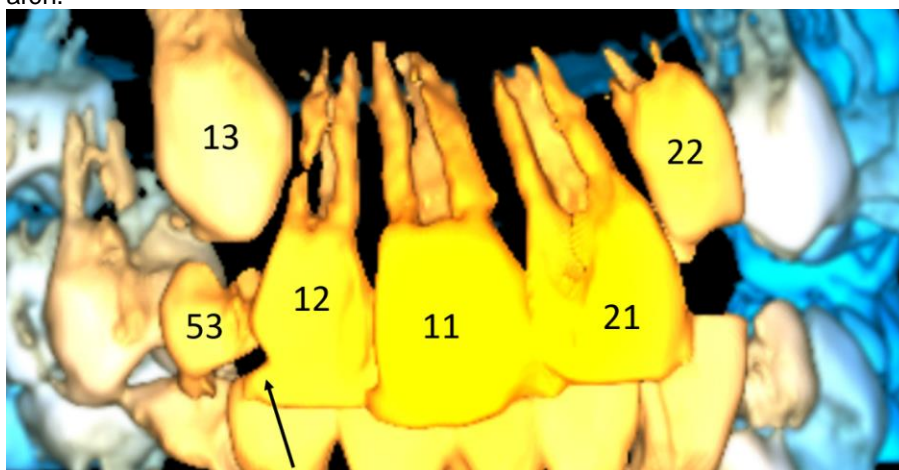
281
282
283

284 Step 2. 3D dental tissue reconstruction: we describe the dental arch tooth by tooth.



285

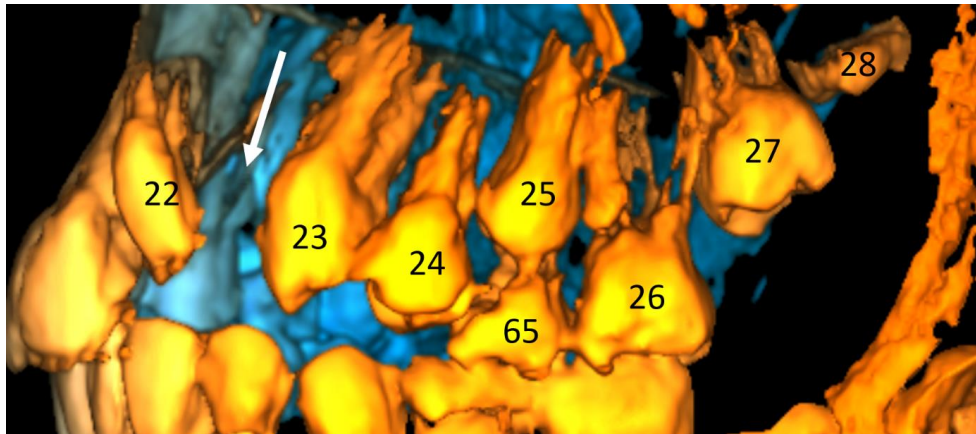
286 **Fig. 2. 3D reconstruction.** Right lateral view. Germ bud of tooth n°18
 287 deeply non-erupted, tooth n°17 non-erupted, tooth n°16 on the arch, tooth
 288 n°55 on the arch, tooth n°15 non-erupted, with the crown surrounded by the
 289 roots of the tooth n°55, tooth n°14 on the arch, tooth n°53 on the arch, tooth
 290 n°13 vestibular and non-erupted, tooth n°12 on the arch, tooth n°11 on the
 291 arch.



292

293 **Fig. 3. 3D reconstruction.** Anterior view. Tooth n°12 on the arch. There
 294 exists a malformation of the distal face of the crown (black arrow). Tooth
 295 n°11 on the arch. Tooth n°21 on the arch. Tooth n°22 impacted.

296 Non-erupted teeth mean that teeth are on the normal path of eruption. Impacted
297 tooth means that the tooth is blocked in its pathway of eruption or there exists a
298 delay in eruption relatively to the chronological age of the patient.
299



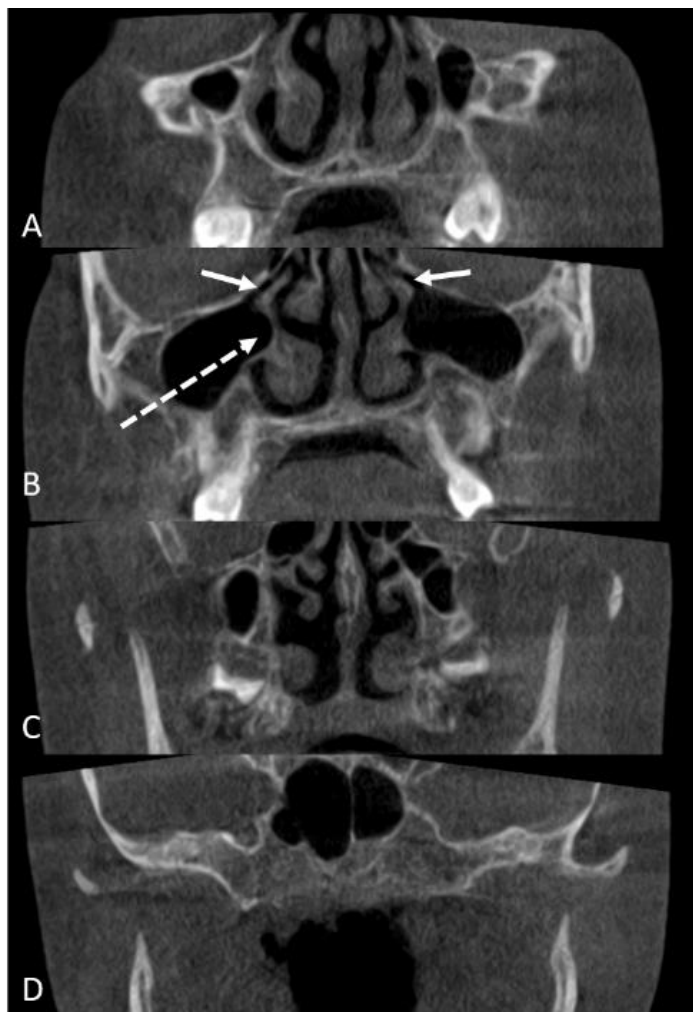
300

301 **Fig. 4. 3D reconstruction.** Left lateral view. Tooth n°22 impacted. The
302 crown is oriented toward the palate in sagittal view. Tooth n°23 on the arch.
303 Tooth n°24 on the arch. Tooth n°65 on the arch. Tooth n°25 non-erupted,
304 with the crown surrounded by the roots of the tooth n°65. Tooth n°26 on the
305 arch. Tooth n°27 non-erupted. Tooth n°28 deeply non-erupted. Arrow:
306 alveolar cleft (lack of 3D reconstruction of a thin bone).
307

308 The 3D reconstruction of dental tissues does not allow to visualize alveolar bone
309 graft and should not be used for that purpose. Only axial slices allow to evaluate the
310 bony remnants of the alveoloplasty (Figure 1).
311

312
313
314
315
316
317
318
319
320
321
322
323
324
325
326

327 Step 3. Coronal view: we search for cleft palate pathway and its extension; we
328 describe any anomaly in maxillary, ethmoid and sphenoid sinuses if existing.
329



330

331 **Fig. 5. 2D coronal view.** A. No anomalies on the anterior view of right and
332 left maxillary sinus. B. Area of ostium and infundibulum of right and
333 left maxillary sinus (arrows). Pneumatisation of the root of the right inferior
334 turbinate (dotted arrow). C. No anomalies on the posterior view of right and
335 left maxillary sinus. D. No anomalies on the sphenoid sinus area. A-C: No
336 presence of right/left cleft palate. A-C: No deviation of nasal septum.

337

338

339 Step 4. Sagittal and coronal view: we check the opening (calcification sites) of the
340 sphenoccipital synchondrosis, and we are checking potential anomalies/variations
341 of the occipital bone.
342



343

344 **Fig. 6. 2D view of sphenoccipital synchondrosis.** A. sagittal view.
345 Opened sphenoccipital synchondrosis (arrows). B. Coronal view. Opened
346 sphenoccipital synchondrosis (arrows).

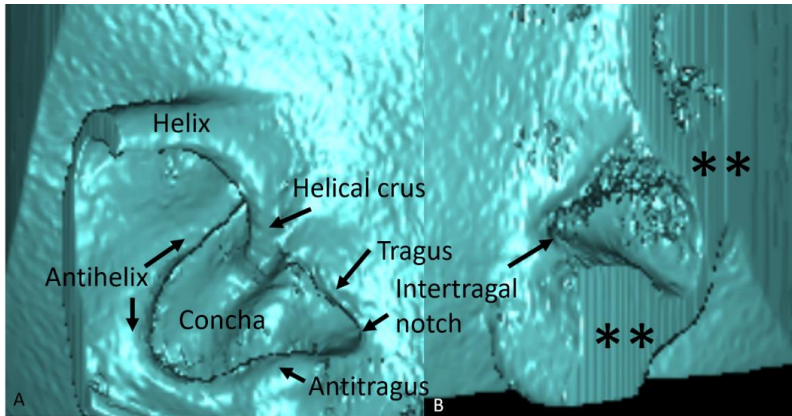
347

348 Step 5. 3D bone tissue reconstruction: we search for C1-C2 vertebra anomalies.
349 For this patient there were no anomalies related to the C1-C2 vertebra.

350

351 Step 6. 3D soft tissue reconstruction: we search for external ear anomalies.

352



353

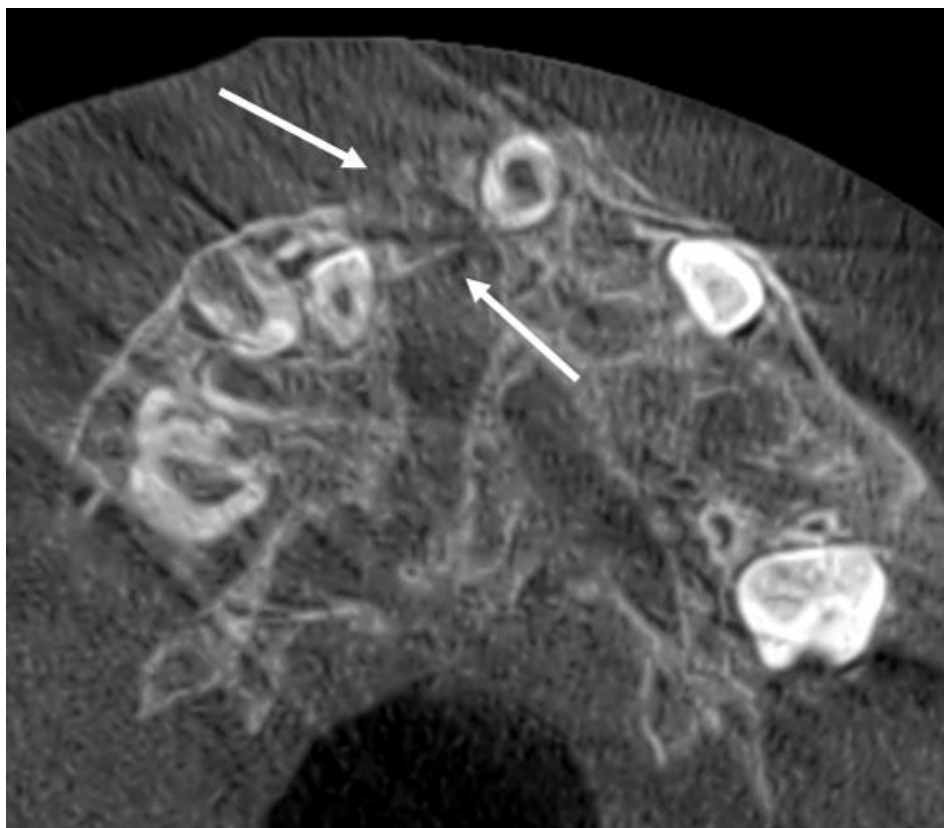
354 **Fig. 7. 3D soft tissue external ear reconstruction.** A. Right external ear.
355 Outer part of the helix is out of the field of view. Presence of deep intertragal
356 notch, and erasure of tragus. B. Left external ear. ** Left external ear is
systematically outside the field of view.

357
358

2. Patient 7 years-old, right cleft lip palate, 6 months postoperative control

359
360
361

Step 1. Axial view: we search for presence or absence of bone bridge remnants of alveolar bone graft (iliac crest).

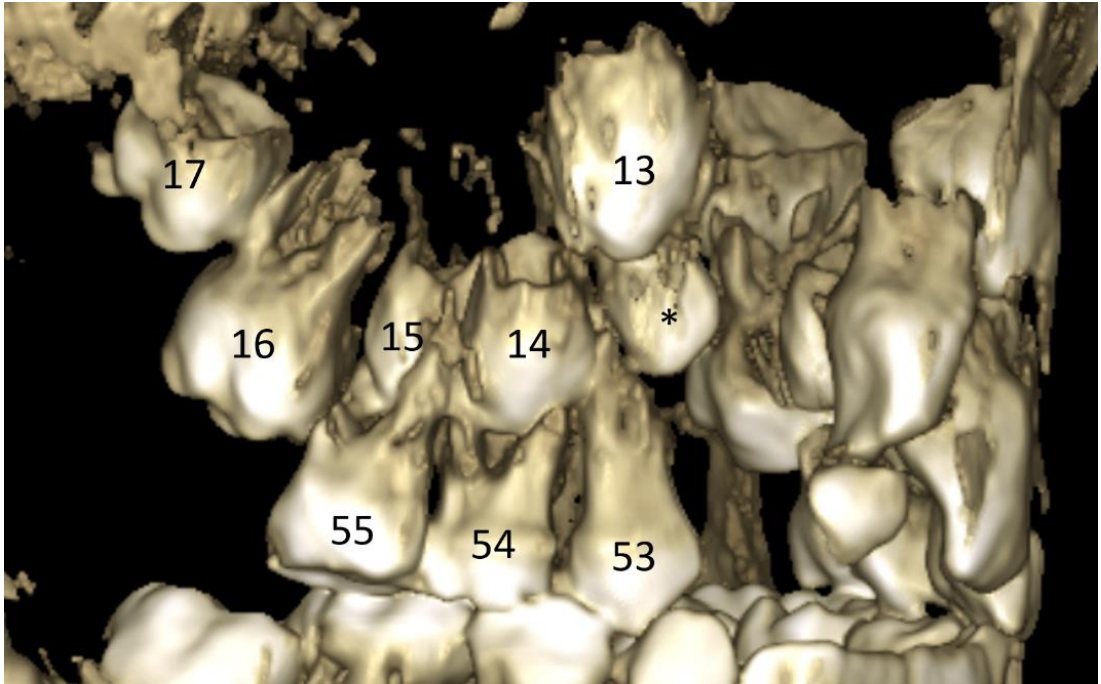


362

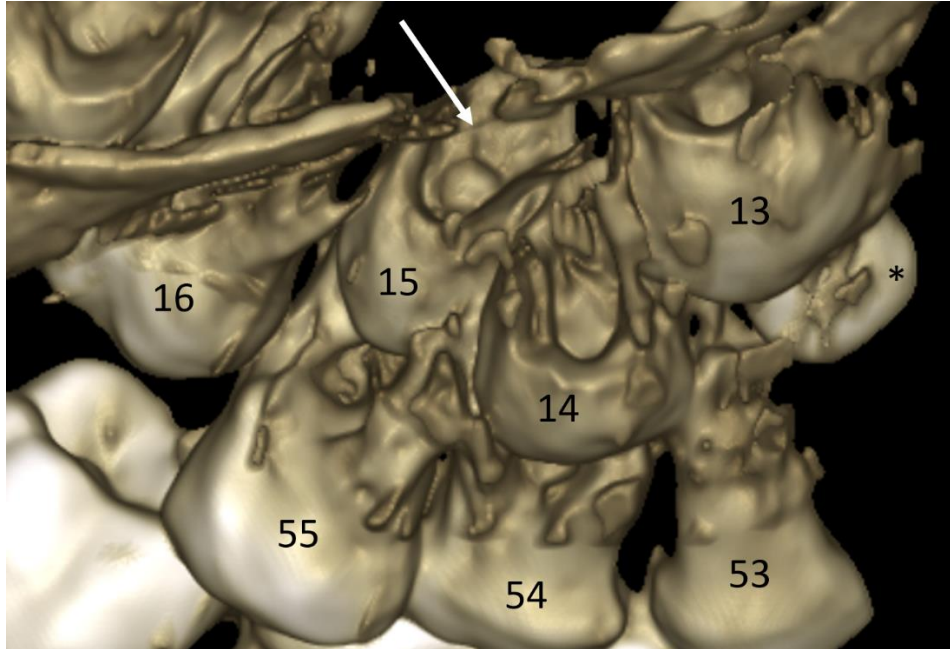
Fig. 8. Axial view. Arrows: presence of large bone bridge of alveolar bone graft between teeth n°13 and n°11.

363
364
365
366
367
368
369
370
371
372
373

374 Step 2. 3D dental tissue reconstruction: we describe the dental arch tooth by tooth.
375



376
377 **Fig. 9. 3D reconstruction.** Right lateral view. Germ bud of tooth n°17
378 deeply non-erupted. Tooth n°16 non-erupted. Tooth n°55 on the arch. Germ
379 bud of tooth n°15 non-erupted, surrounded by the roots of the tooth n°55,
380 and slightly displaced to palatine side. Tooth n°54 on the arch. Germ bud of
381 tooth n°15 non-erupted, surrounded by the roots of the tooth n°54. Tooth
382 n°53 on the arch. *Supernumerary tooth mesial to the apex of the tooth n°53
383 and occlusal to the crown of the tooth n°13. Tooth n°13 non-erupted and
384 vestibular. Agenesis of the tooth n°12. Lack of 3D reconstruction of existing
385 alveolar bone bridge between teeth n°13 and n°11.
386
387
388
389
390
391
392
393
394



395

396

397

398

399

400

401

402

403

404

405

406

407

408

409

410

411

412

413

414

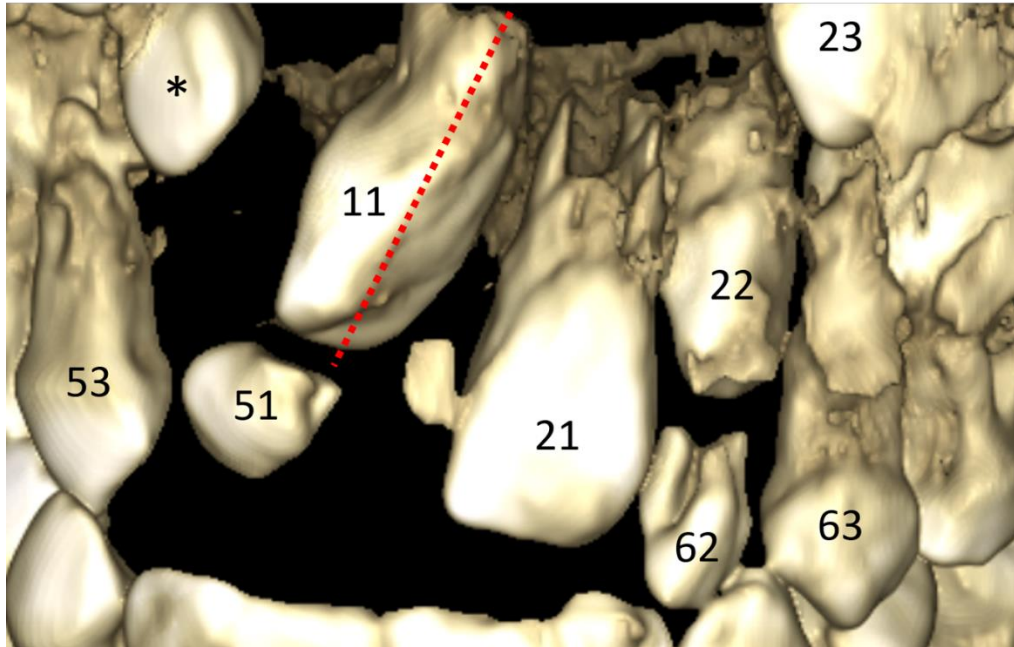
415

416

417

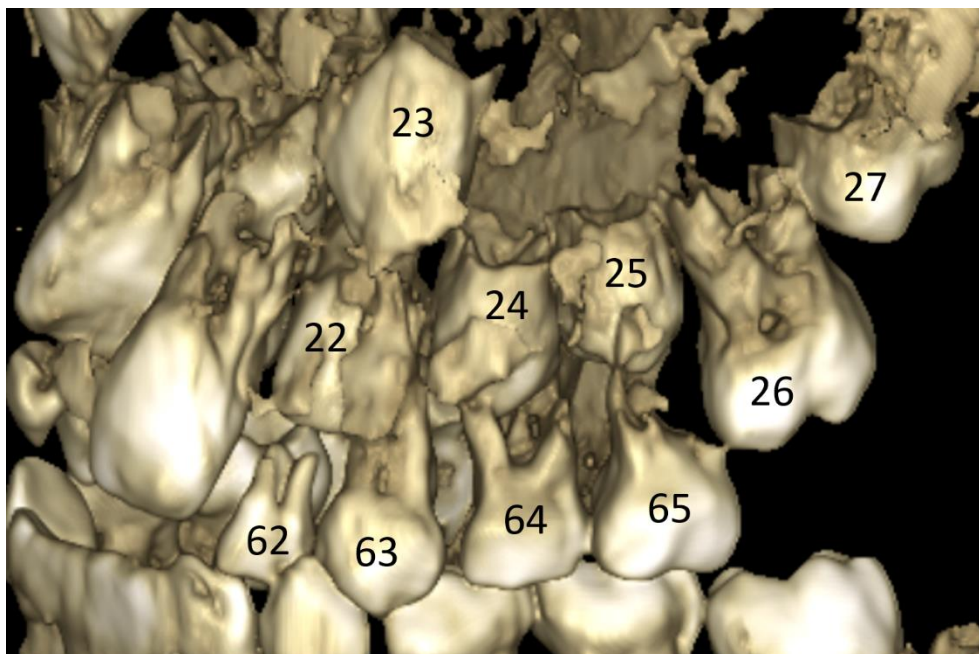
418

Fig. 10. 3D reconstruction. Right lateral and upper view. Germ bud of tooth n°15 non-erupted, surrounded by the roots of the tooth n°55, and slightly displaced to palatine side.



419
420
421
422
423
424
425
426
427
428
429
430
431
432
433
434
435
436
437
438
439
440
441

Fig. 11. 3D reconstruction. Anterior view. Tooth n°53 on the arch. *Supernumerary tooth mesial and close to the apex of the tooth n°53. Agenesis of the tooth n°12. Tooth n°51 on the arch. Tooth n°11 non-erupted with rotation along its main axis (red dotted line). The distal face of the tooth n°11 is directed to the vestibular side. Tooth n°21 on the arch. Tooth n°62 on the arch. Tooth n°22 non-erupted. Tooth n°63 on the arch. Tooth n°23 non-erupted and apical to the apex of the tooth n°63.



442

443 **Fig. 12. 3D reconstruction.** Left lateral view. Tooth n°62 on the arch. Tooth
444 n°22 non-erupted. Tooth n°63 on the arch. Tooth n°23 non-erupted apical to
445 the apex of the root of the tooth n°63. Tooth n°64 on the arch. Germ bud of
446 the tooth n°24, non-erupted, slightly displaced to mesial in relation with the
447 roots of the tooth n°64. Tooth n°65 on the arch. Germ bud of the tooth n°25,
448 non-erupted, slightly displaced to mesial in relation with the roots of the tooth
449 n°65. Tooth n°26 non-erupted. Tooth n°27 deeply non-erupted.

450

451

452

453

454

455

456

457

458

459

460

461

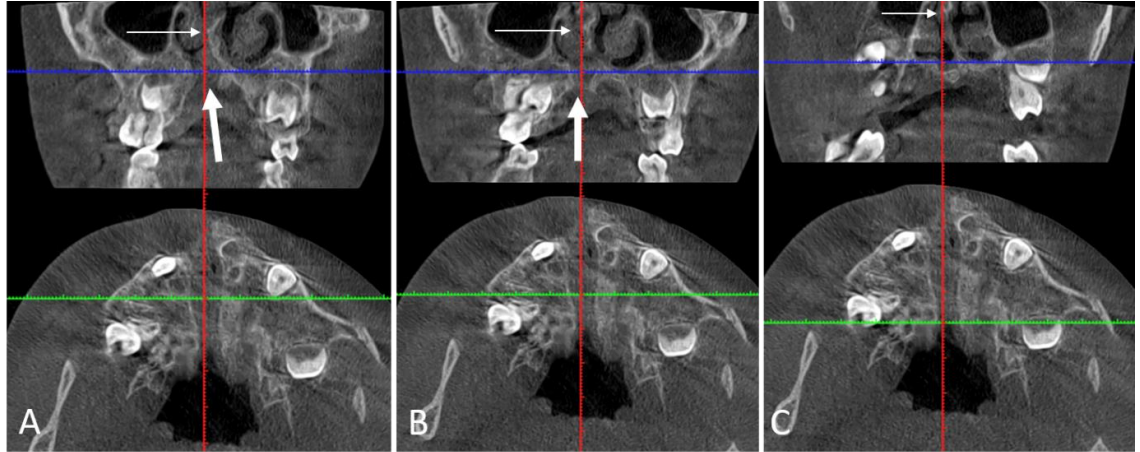
462

463

464

465

466 Step 3. Coronal view: we search for cleft palate pathway and its extension; we
467 describe any anomaly in maxillary, ethmoid and sphenoid sinuses if existing.
468



469

470 **Fig. 13. Coronal (upper) and axial (lower) view.** A. First premolar area. On
471 the coronal view: thin arrow: deviation of the nasal septum to the right. Thick
472 arrow: Right cleft palate in the area of the first premolar. B. Second premolar
473 area. On the coronal view: thin arrow: deviation of the nasal septum to the
474 right. Thick arrow: Right cleft palate in the area of the second premolar. C.
475 First molar area. On the coronal view: thin arrow: deviation of the nasal
476 septum to the right. Absence of the right cleft palate in the in the area of the
477 first molar.

478
479
480
481
482
483
484
485
486
487
488
489
490
491
492
493
494
495

496 Step 4. Sagittal and coronal views: we check the opening (calcification sites) of the
497 sphenooccipital synchondrosis, and we are checking potential anomalies/variations
498 of the occipital bone.
499



500

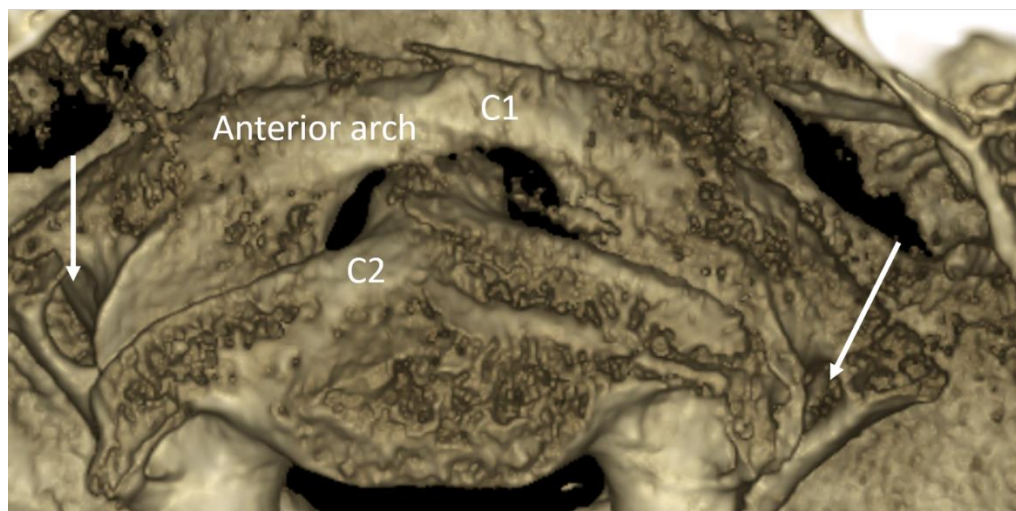
501 **Fig. 14. Sagittal view.** Opened sphenooccipital synchondrosis (arrows).

502

503

504

Step 5. 3D bone tissue reconstruction: we search for C1-C2 vertebra anomalies.



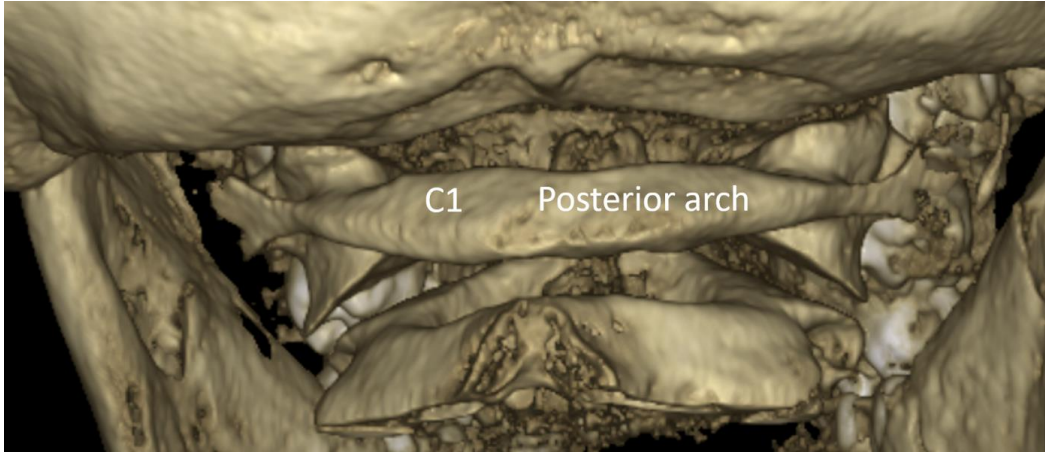
505

506

507

508

Fig. 15. 3D reconstruction of C1 and C2 vertebra. Anterior view. Normal and complete anterior arch of C1 vertebra. Arrows: Transverse foramen for right and left vertebral artery.



509
510
511
512
513
514
515

Fig. 16. 3D reconstruction of C1 and C2 vertebra. Posterior view. Normal and complete posterior arch of C1 vertebra.

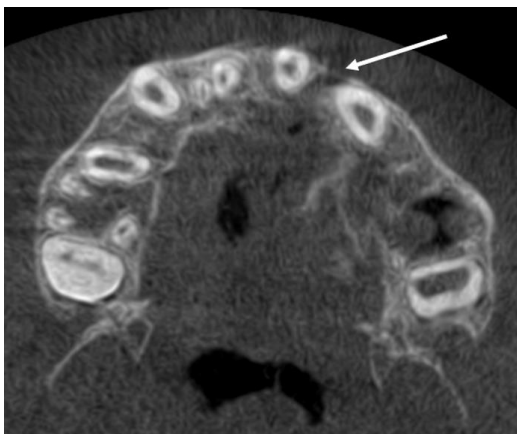
Step 6. 3D soft tissue reconstruction: we search for external ear anomalies. We found no anomalies of external ears in this patient.

516
517

3. Patient 10 years-old, left cleft lip palate, 6 months postoperative control

518
519
520

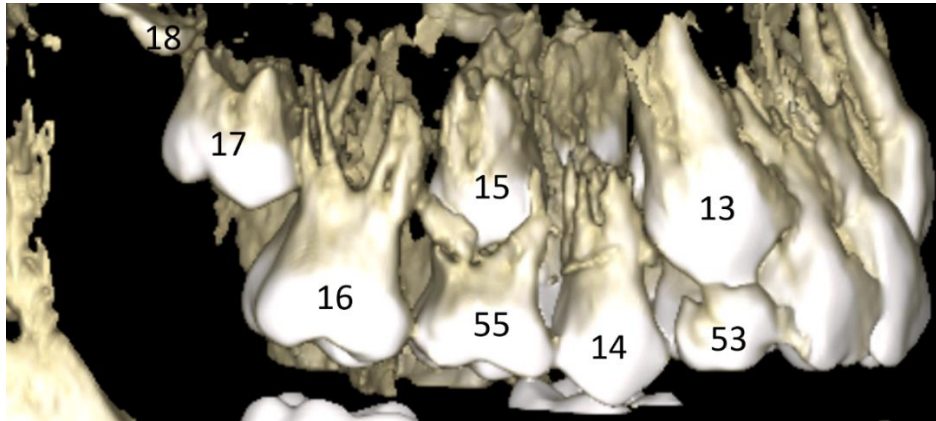
Step 1. Axial view: we search for presence or absence of bone bridge remnants of alveolar bone graft (iliac crest).



521
522
523
524

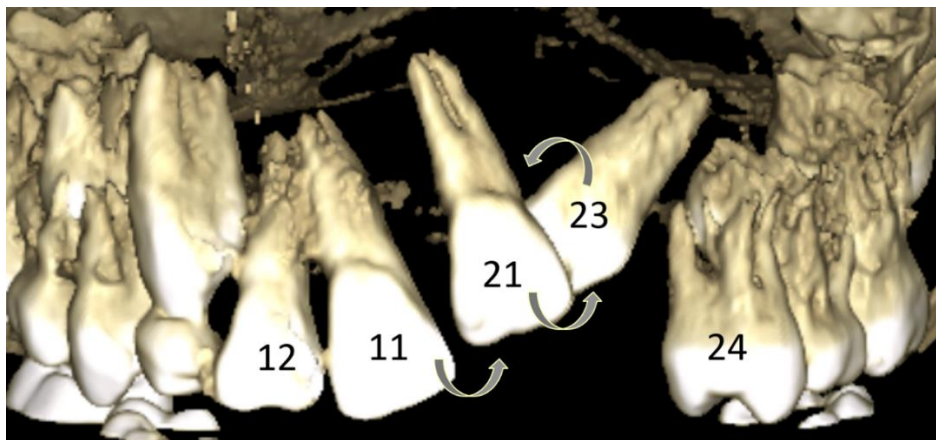
Fig. 17. Axial view. Arrow: presence of thin bone bridge of alveolar bone graft between teeth n°21 and n°23.

525 Step 2. 3D dental tissue reconstruction: we describe the dental arch tooth by tooth.
526



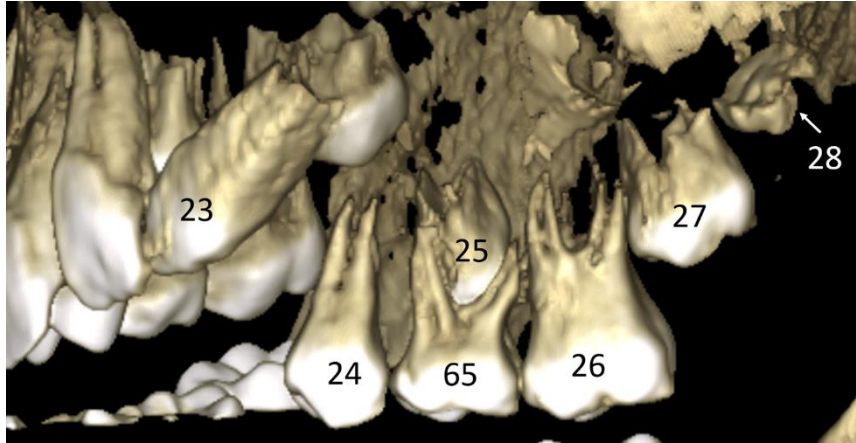
527

528 **Fig. 18. 3D reconstruction.** Right lateral view. Germ bud of tooth n°18
529 deeply non-erupted. Tooth n°17 non-erupted. Tooth n°16 on the arch. Tooth
530 n°55 on the arch. Tooth n°15 non-erupted, and surrounded by the roots of
531 the tooth n°55. Tooth n°14 on the arch. Tooth n°53 on the arch. Tooth n°13
532 non-erupted with the crown inside the tooth n°53.
533



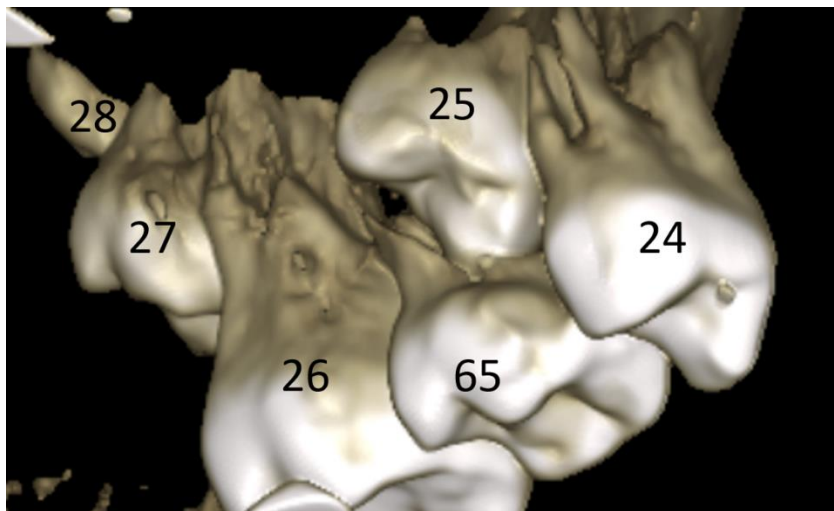
534

535 **Fig. 19. 3D reconstruction.** Anterior and left lateral view. Tooth n°11 tilted
536 toward left side and toward midline (rounded arrow). Tooth n°21 tilted toward
537 left side (rounded arrow). Agenesis of the tooth n°22. Tooth n°23 tilted
538 toward right side (rounded arrow).



539
540
541
542
543
544

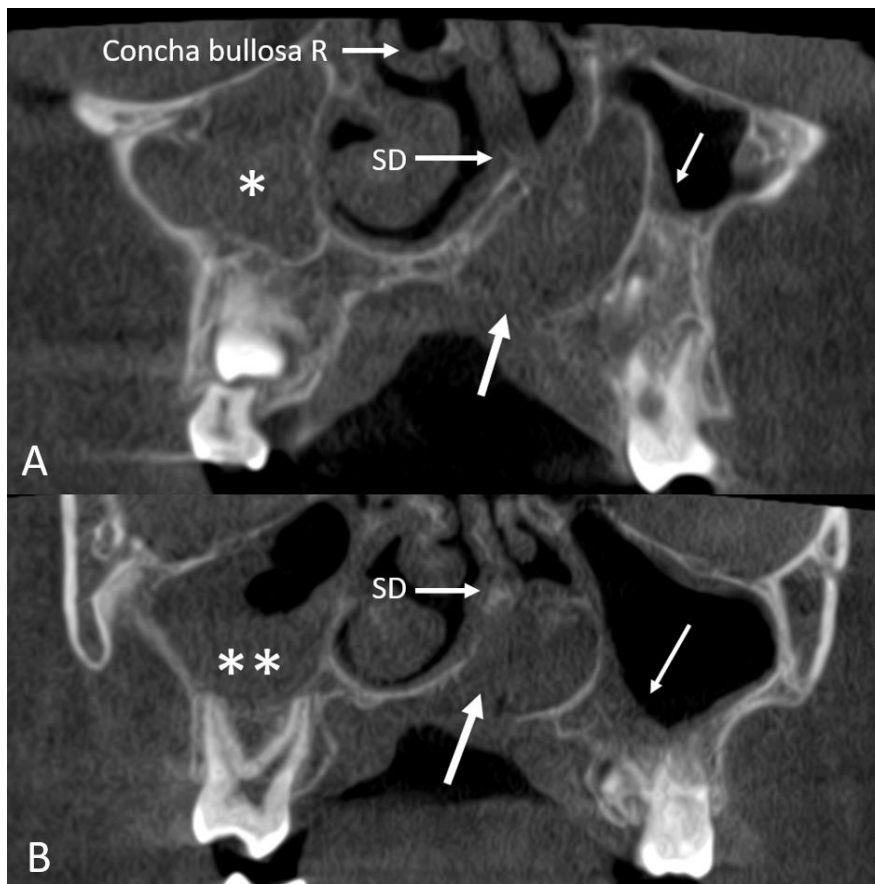
Fig. 20. 3D reconstruction. Left lateral view. Tooth n°24 on the arch. Tooth n°65 on the arch. Tooth n°25 non-erupted, and surrounded by the roots of the tooth n°65. Tooth n°26 on the arch. Tooth n°27 non-erupted. Germ bud of tooth n°28 deeply non-erupted.



545
546
547
548
549
550
551
552
553

Fig. 21. 3D reconstruction. Left lateral and palatine view. Tooth n°25 displaced toward the palate.

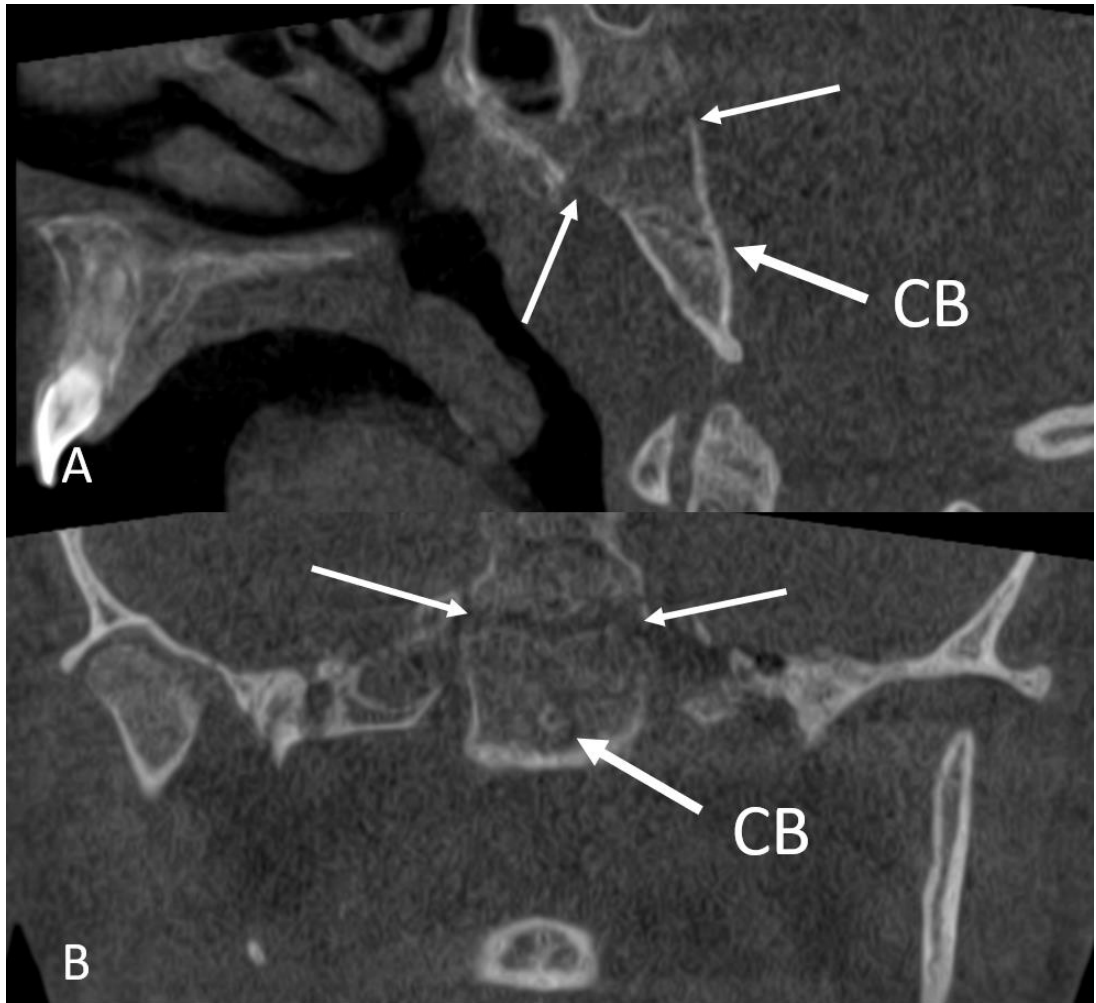
554 Step 3. Coronal view: we search for cleft palate pathway and its extension; we de-
 555 scribe any anomaly in maxillary, ethmoid and sphenoid sinuses if existing.
 556



557

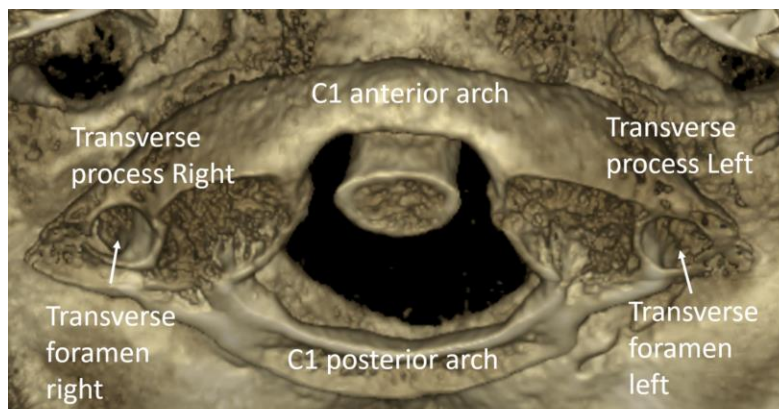
558 **Fig. 22. Coronal view.** A. Area of the tooth n°15. Cleft of the left nasal floor
 559 (thicker arrow). SD: nasal septum deviation toward left, and toward cleft
 560 palate. Right concha bullosa. * Total filling of the right maxillary sinus.
 561 Thinner arrow: thickening of the mucosa of the left maxillary sinus. B. Area of
 562 the tooth n°16. Cleft of the left nasal floor (thicker arrow). SD: nasal septum
 563 deviation toward left, and toward cleft palate. ** Important thickening of the
 564 mucosa of the right maxillary sinus. Thinner arrow: thickening of the mucosa
 565 of the left maxillary sinus.
 566
 567
 568

569 Step 4. Sagittal and coronal view: we check the opening (calcification sites) of the
570 sphenooccipital synchondrosis, and we check potential anomalies/variations of the
571 occipital bone.
572



573 **Fig. 23. A. Sagittal view.** Arrows: opened sphenooccipital synchondrosis.
574 CB: diagonal canal basilaris. B. Coronal view. Arrows: opened
575 sphenooccipital synchondrosis. CB: unique median canal basilaris.
576
577
578
579
580

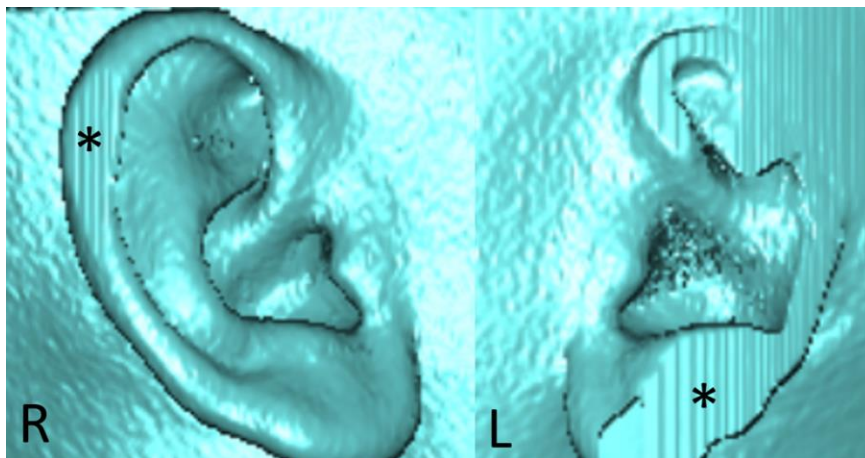
581 Step 5. 3D bone tissue reconstruction: we search for C1-C2 vertebra anomalies.
 582



583

584 **Fig. 24. 3D reconstruction of C1 vertebra.** Normal anatomy of C1
 585 vertebra. Complete anterior and posterior arch, and complete anterior and
 586 posterior walls of the transverse foramen right and left.
 587

588 Step 6. 3D soft tissue reconstruction: we search for external ear anomalies. We
 589 found no anomalies of external ears in this patient.
 590



591

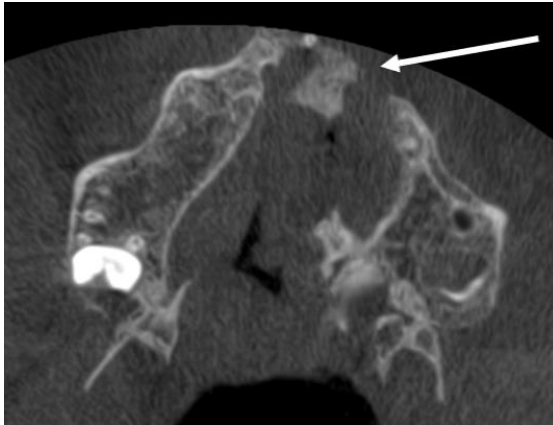
592 **Fig. 25. 3D reconstruction of ears.** R. Right ear with normal anatomy and
 593 almost complete (*area outside the field of view). L. left ear. *Major part of
 594 the left ear is situated outside of the field of view.
 595
 596

597
598

4. Patient 13 years-old, left cleft lip palate, evaluation of the remaining alveolar graft

599
600
601

Step 1. Axial view: we search for presence or absence of bone bridge remnants of alveolar bone graft (iliac crest).

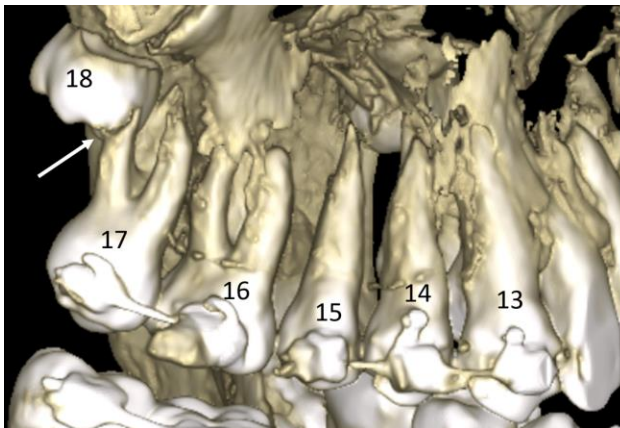


602

603
604
605
606
607

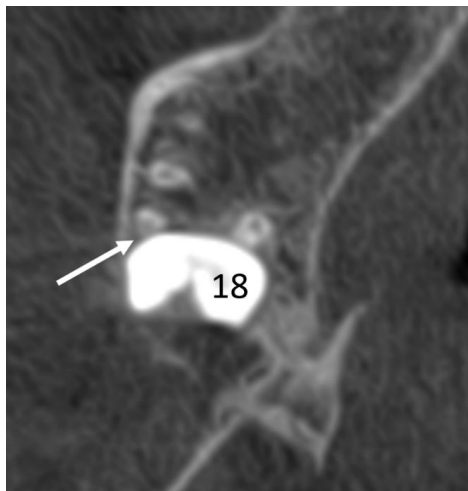
Fig. 26. Axial view. Absence of the bone wall between the fragments of the left upper maxilla (arrow).

Step 2. 3D dental tissue reconstruction: we describe the dental arch tooth by tooth.



608
609
610
611
612
613

Fig. 27. 3D reconstruction. Right lateral view. Germ bud of tooth n°18 deeply non-erupted. Possible external resorption of the distovestibular root of the tooth n°17 by the tooth n°18. Tooth n°17 on the arch. Tooth n°16 on the arch. Tooth n°15 on the arch. Tooth n°14 on the arch. Tooth n°14 on the arch. Tooth n°13 on the arch.



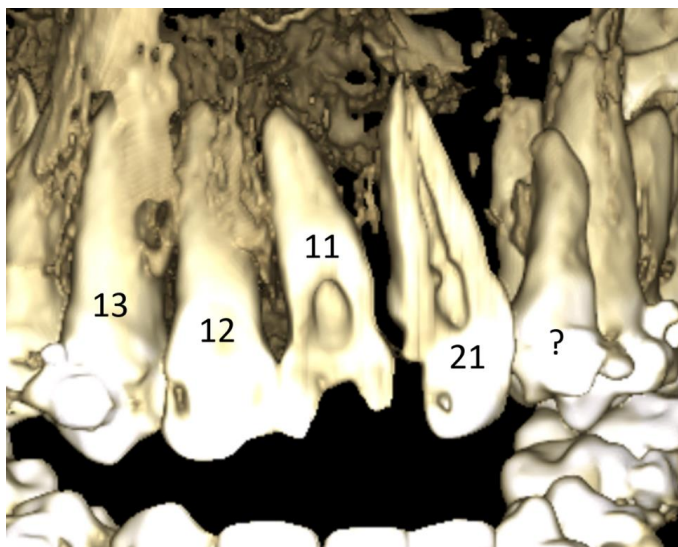
614

615

616

617

Fig. 28. Axial view. External resorption of the distovestibular root of the tooth n°17 by the tooth n°18 (arrow).



618

619

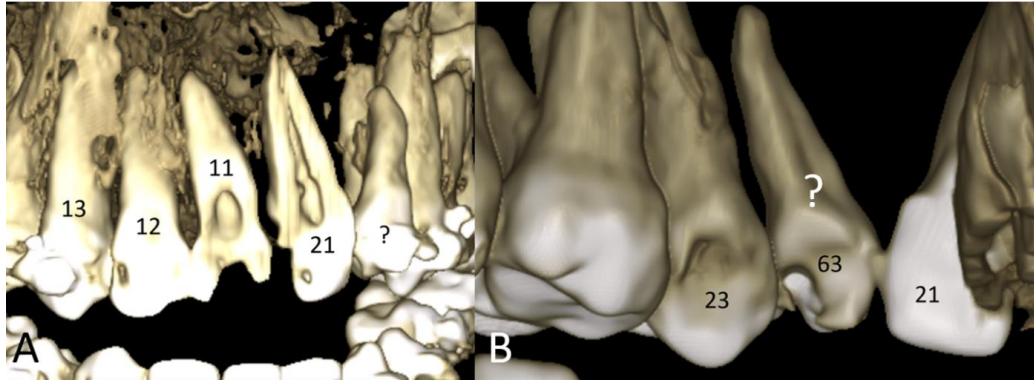
620

621

622

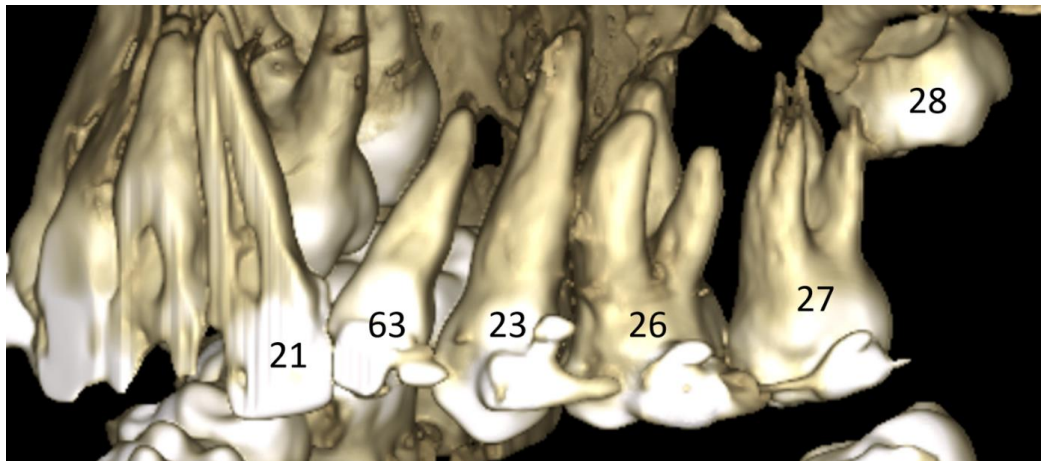
623

Fig. 29. 3D reconstruction. Anterior view. Tooth n°13 on the arch. Tooth n°12 on the arch. Tooth n°11 on the arch. Tooth n°21 on the arch. Slicing of the crowns and roots of teeth n°11 and 21 because the teeth are partially situated outside of the field of view. ? Need of more than one 3D reconstruction view to determine the numbering of this tooth.



624
625
626
627
628
629

Fig. 30. A. 3D reconstruction. Anterior view. ? undetermined numbering of the tooth lateral to tooth n°21. B. 3D reconstruction. Palatine view. ? is related to the not resorbed tooth n°63 which is situated between teeth n°21 and 23.

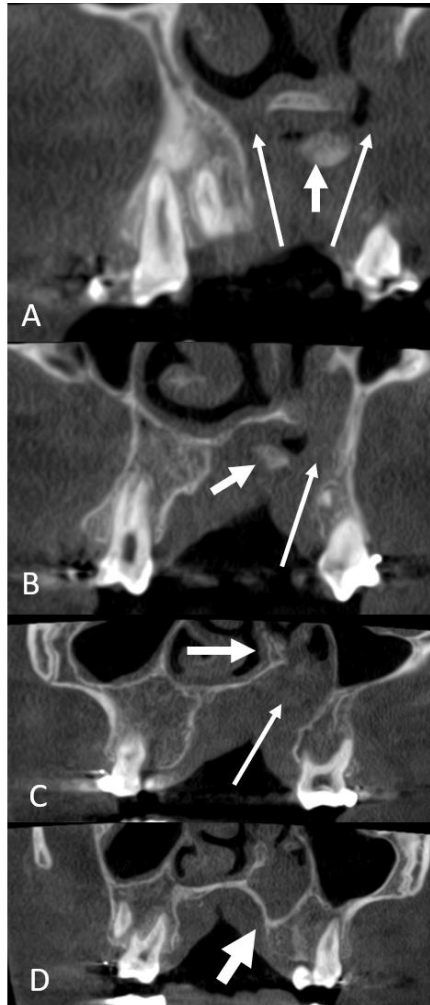


630

631
632
633
634
635
636
637
638
639
640

Fig. 31. 3D reconstruction. Left lateral view. Tooth n°21 on the arch. Tooth n°63 tilted to the right. Tooth n°23 on the arch and in transmigration positioned laterally to the tooth n°63. Agenesis of tooth n°24. Agenesis of the tooth n°25. Tooth n°26 on the arch. Tooth n°27 on the arch. Germ bud of tooth n°28 deeply non-erupted.

641 Step 3. Coronal view: we search for cleft palate pathway and its extension; we de-
 642 scribe any anomaly in maxillary, ethmoid and sphenoid sinuses if existing.
 643



644 **Fig. 32. Coronal view.** A. Anterior area. Bilateral cleft palate (thin arrows).
 645 Remnants of the alveolar bone bridge/graft (thick arrow). B. Premolar area.
 646 Left cleft palate (thin arrow). Remnants of the alveolar bone bridge/graft
 647 (thick arrow). C. First molar area. Left cleft palate (thin arrow). Deviation of
 648 nasal septum toward left (thick arrow). D. Second molar area. No cleft
 649 palate. Left nasal fossa is deeper than the right nasal fossa (thick arrow).
 650 Right cleft palate is limited to the anterior and premolar area. Left cleft palate
 651 is extended between anterior and first molar area.
 652
 653

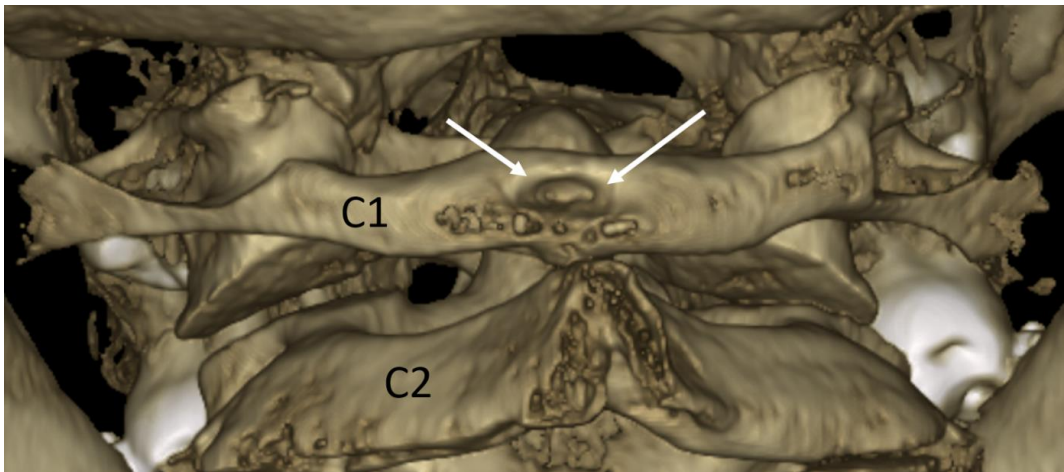
654 The right cleft palate is situated between the anterior and the premolar area. The left
655 cleft palate is extended between anterior and first molar area (Figure 32).

656
657 Step 4. Sagittal and coronal view: we check the opening (calcification sites) of the
658 sphenoccipital synchondrosis, and we check potential anomalies/variations of the
659 occipital bone.
660

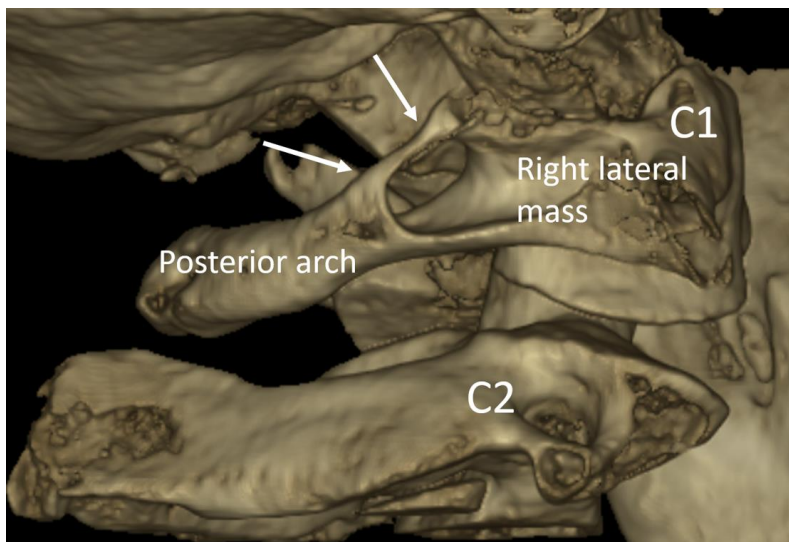


661
662 **Fig. 33. Sagittal view.** Arrows: opened sphenoccipital synchondrosis (thin
663 arrow). Center of calcification present on the retropharyngeal side of the
664 clivus (thick arrow).
665

666 Step 5. 3D bone tissue reconstruction: we search for C1-C2 vertebra anomalies.
667

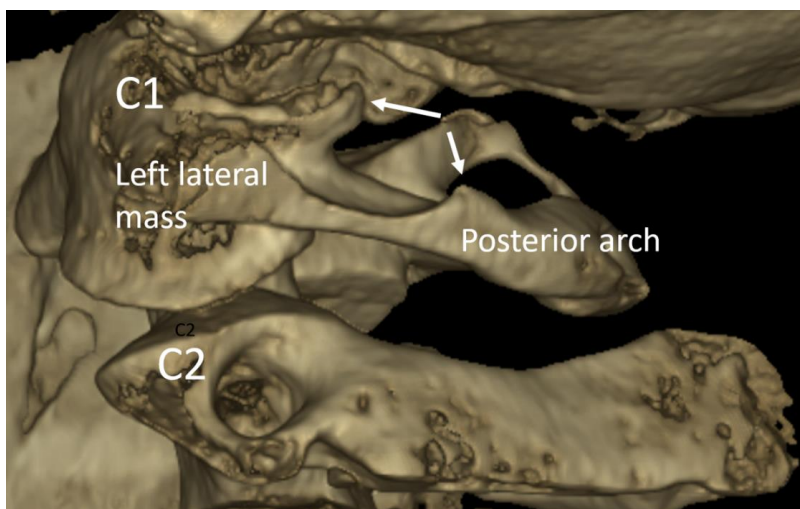


668
669 **Fig. 34. 3D reconstruction.** Posterior view of the C1 and C2 vertebra.
670 Recess in the posterior arch of C1 on the midline (thin arrows).



671
672
673
674
675

Fig. 35. 3D reconstruction. Right lateral view of C1 and C2 vertebrae. Complete ponticulus posticus (arrows) between the right lateral mass and the right posterior arch.



676
677
678
679
680
681

Fig. 36. 3D reconstruction. Left lateral view of C1 and C2 vertebrae. Partial ponticulus posticus (arrows) between the left lateral mass and the left posterior arch.

682 Step 6. 3D soft tissue reconstruction: we search for external ear anomalies. We
683 found no anomalies of external ears in this patient.

684
685 There were no anomalies of external ears for this patient.
686

687 **5. Patient 7 years-old, left cleft lip palate, evaluation**
688 **before surgery**

689 Step 1. Axial view: we search for presence or absence of bone bridge remnants of
690 alveolar bone graft (iliac crest).
691

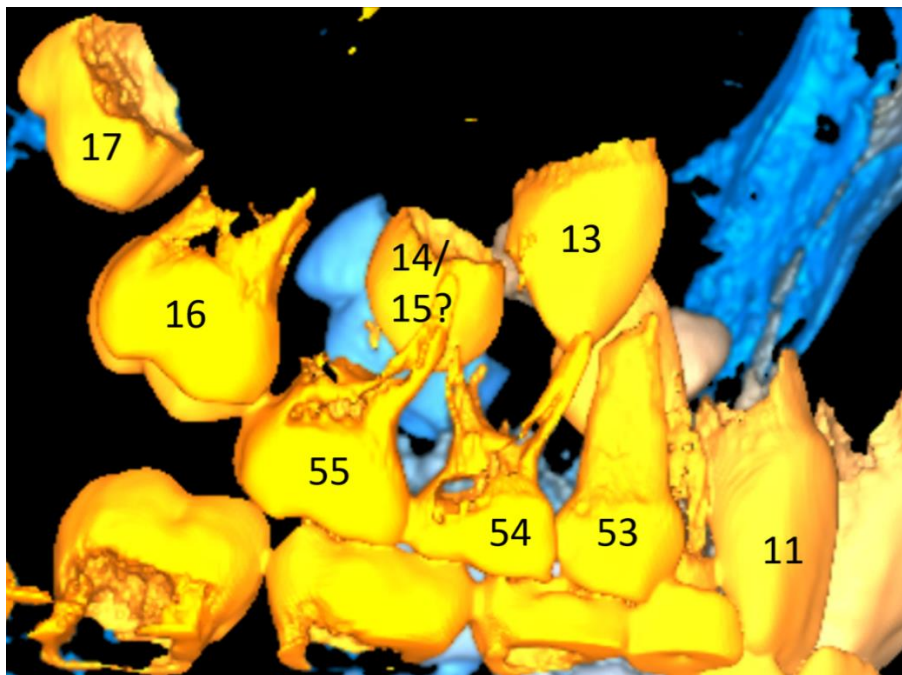


692
693 **Fig. 37. Axial view.** Left alveolar cleft between the fragments of the upper
694 maxilla (arrow).
695

696
697
698
699
700
701
702

703
704

Step 2. 3D dental tissue reconstruction: we describe the dental arch tooth by tooth.



705
706
707
708
709
710
711
712
713
714
715
716
717
718
719
720
721
722
723
724
725
726

Fig. 38. 3D reconstruction. Right lateral view. Germ bud of tooth n°17 deeply non-erupted. Tooth n°16 non-erupted. Tooth n°55 on the arch. Tooth n°54 on the arch. Agenesis of the tooth n°14 or n°15, and presence of only one premolar germ bud between the mesial roots of the tooth n°55 and between the distal roots of the tooth n°54. Tooth n°53 on the arch. Tooth n°13, non-erupted, with its crown distoapical to the apex of the tooth n°53.

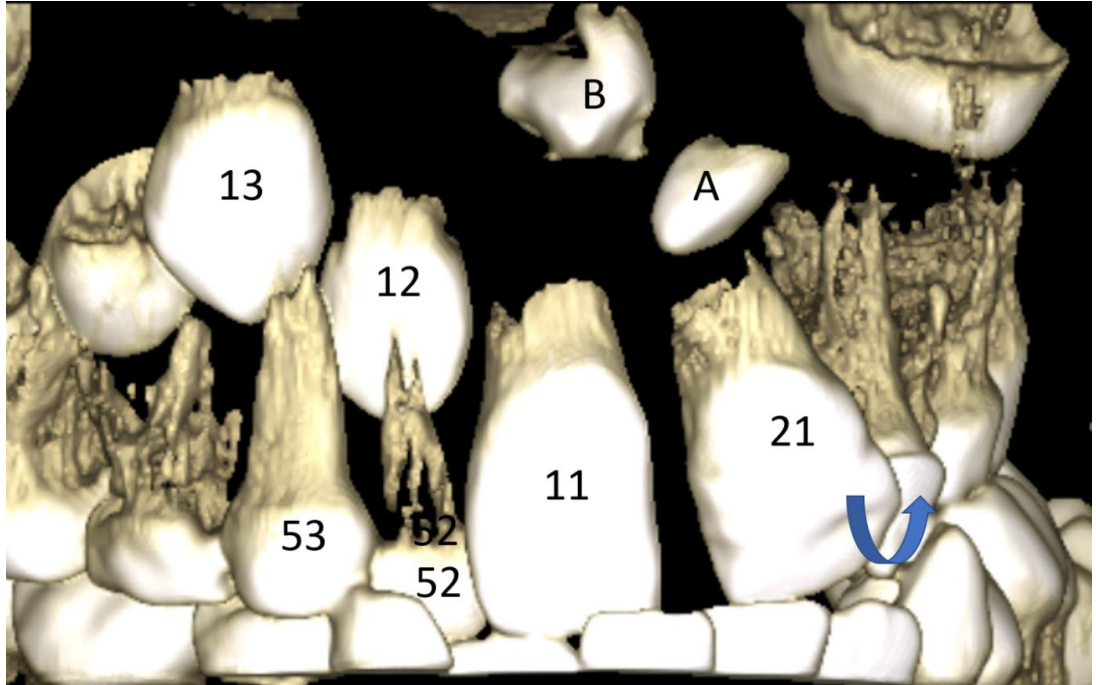


Fig. 39. 3D reconstruction. Anterior view. Tooth n°53 on the arch. Tooth n°13 non-erupted, with its crown distoapical to the apex of the tooth n°53. Tooth n°52 on the arch. Tooth n°12 non-erupted, palatine to the tooth n°52. Tooth n°11 in the arch. Tooth n°21 on the arch and tilted toward left (rounded arrow). A and B: presence of two supernumerary teeth on the left edge of the alveolar cleft.

727
728
729
730
731
732
733
734
735
736
737
738
739
740
741
742
743
744
745
746
747
748
749

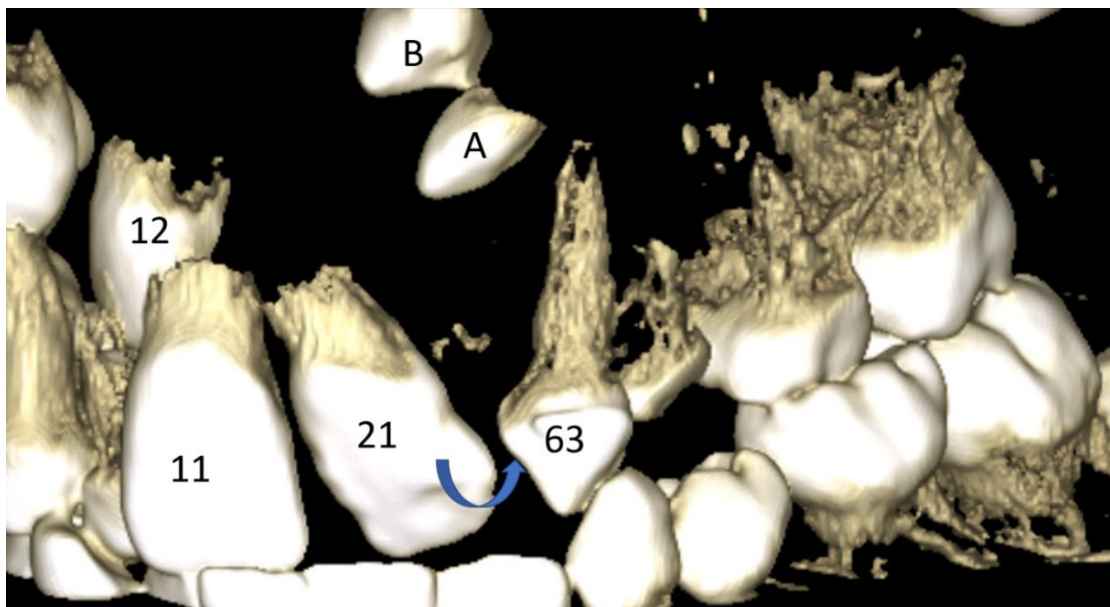
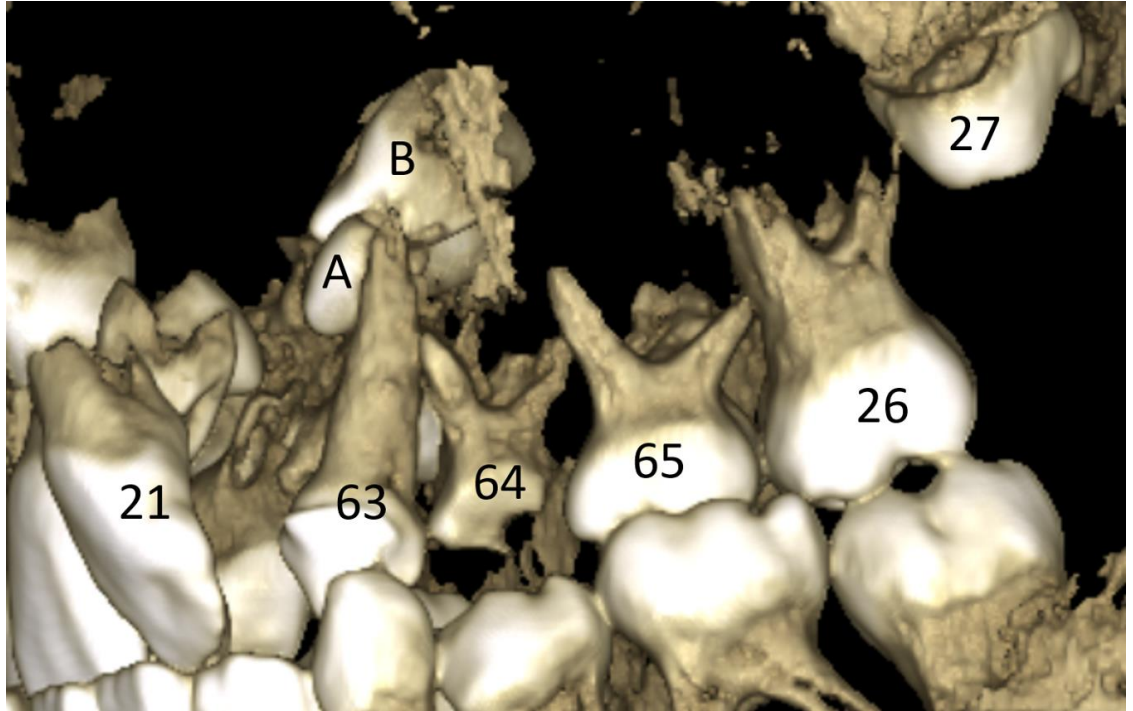


Fig. 40. 3D reconstruction. Left lateral view. Tooth n°21 on the arch, tilted toward left (rounded arrow), and rotated to the palatine side. A and B: presence of two supernumerary teeth on the left edge of the alveolar cleft. Tooth n°63 on the arch with rotation of the tooth along its main axis. The mesial side of the tooth is rotate toward vestibular side. Agensis of teeth n°22 and 23.

750
751
752
753
754
755
756
757
758
759
760
761
762
763
764
765
766
767
768
769
770
771
772
773
774
775



776

777

778

779

780

781

782

783

784

785

786

787

788

789

790

791

792

793

794

795

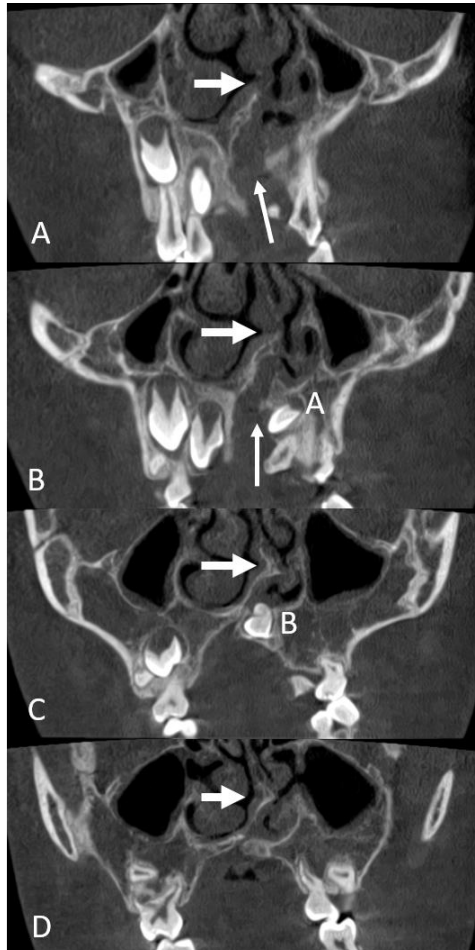
796

797

Fig. 41. 3D reconstruction. Left lateral view. A and B: presence of two supernumerary teeth on the left edge of the alveolar cleft. Tooth n°63 on the arch. Tooth n°64 on the arch. Agenesis of the tooth n°24. Tooth n°65 on the arch. Agenesis of the tooth n°25. Tooth n°26 on the arch. Germ bud of the tooth n°27 deeply non-erupted.

798
799
800

Step 3. Coronal view: we search for cleft palate pathway and its extension; we describe any anomaly in maxillary, ethmoid and sphenoid sinuses if existing.



801
802
803
804
805
806
807
808
809
810
811

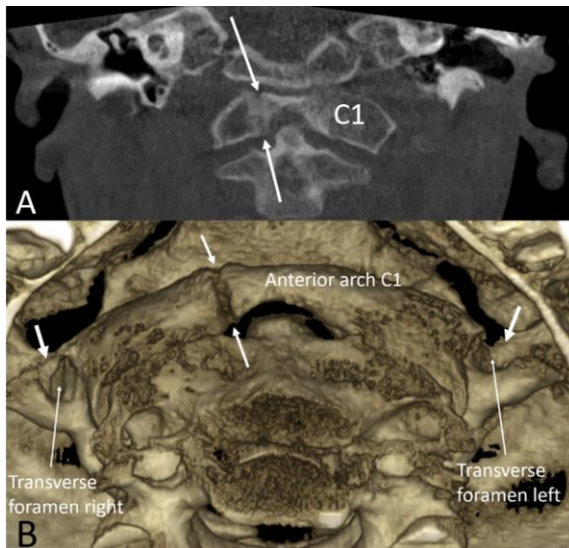
Fig. 42. Coronal view. A. Anterior area. Thin arrow: left cleft palate. Thick arrow: nasal septum deviation toward left. B. Canine area. Thin arrow: left cleft palate narrower than in the anterior area. A: presence of the supernumerary tooth A on the left edge of the cleft palate. Thick arrow: nasal septum deviation toward left. C. Premolar area. Thick arrow: nasal septum deviation toward left with the presence of the bone spur directed toward left. B: presence of the supernumerary geminated tooth A on the left edge of the cleft palate. Cleft palate is closed at this level. D. Thick arrow: nasal septum deviation toward left with the presence of the bone spur directed toward left. No cleft palate at this level.

812 Step 4. Sagittal and coronal view: we check the opening (calcification sites) of the
813 sphenoccipital synchondrosis, and we check potential anomalies/variations of the
814 occipital bone.
815

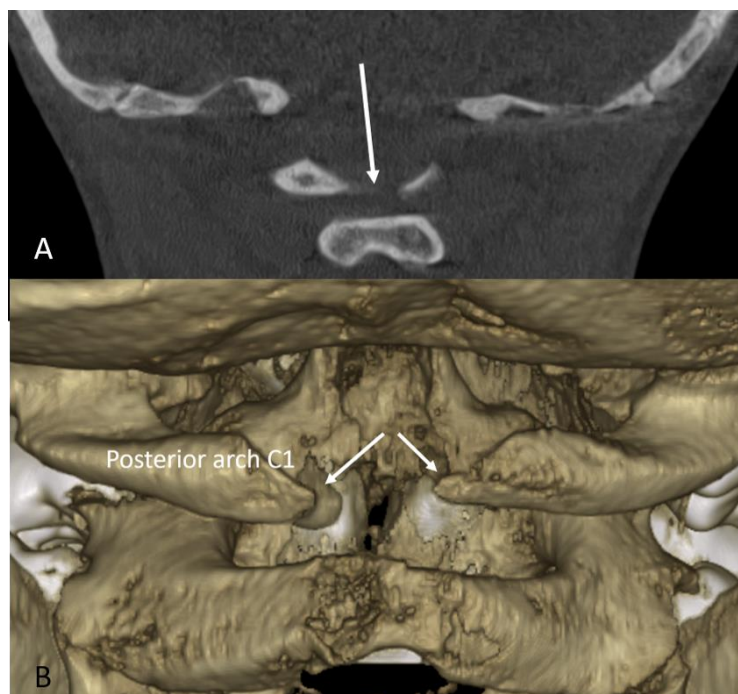


816
817 **Fig. 43. Sagittal view.** Arrows: opened sphenoccipital synchondrosis (thin
818 arrow).
819

820 Step 5. 3D bone tissue reconstruction: we search for C1-C2 vertebra anomalies.
821



822
823 **Fig. 44. A. Coronal view.** Arrows: non fusion of the right neurocentral syn-
824 chondrosis on the anterior arch (normal fusion at the age of 6 years-old). B.
825 3D reconstruction. Anterior view of the C1 vertebra. Arrows: non fusion of
826 the right neurocentral synchondrosis on the anterior arch. Thicker arrows:
827 absence of the anterior wall of the transverse foramen (right and left).
828



829

830 **Fig. 45. Coronal view.** Arrow: absence of the fusion of the posterior arch on
831 the midline. B. 3D reconstruction. Posterior view of the C1 vertebra. Arrows:
832 absence of the fusion of the posterior arch on the midline. Dehiscence
833 between both posterior arches.

834

835 Step 6. 3D soft tissue reconstruction: we search for external ear anomalies. We
836 found no anomalies of external ears in this patient.

837

838 There were no anomalies of external ears for this patient.

839

840

Discussion

841

842 In 2014 Miles et al. stated that 98% radiologists do not learn how to report
843 information from CBCT volume [64]. Therefore, Miles et al proposed their own
844 system of reporting CBCT data in head and neck area to help radiologists communi-
845 cate with other specialties [64]. Similar system was further proposed by Kachlan et
846 al. [65]. However, these systems were not supposed to be used in pediatric nor in
847 CLP patients CBCT examinations. Reporting systems by Miles and Kachlan needed
848 the use of CBCT with large field of view incorporating areas from the skull, through
orbits to the neck area (Table 1). Santos et al., proposed a system of reporting

849 incidental findings on CBCT of CLP patients using most of items of the Miles's
 850 methodology [66]. Santos added the reporting of information from the mandible,
 851 from the orbit, and from the middle and inner ear cavity [66]. Again, a large field of
 852 view is needed to report information from all of these areas. We choose to avoid the
 853 mandible and the orbit in the selected field of view as most indications of use of the
 854 CBCT in CLP patients are related to the maxilla [1-7]. We do not use "Gap" in
 855 Gand classification as this classification of the missing alveolar bone area is too
 856 simplified and subjective (Table 1) [17]. We do not use either "Arch" GAND classi-
 857 fication which corresponds to the discrimination between anterior and posterior
 858 endognathia of the maxilla (Table 1) [17]. We do not use "NasaI" transversal GAND
 859 classification as we describe the sagittal anteroposterior extension of the cleft palate
 860 (Table 1) [17]. We do not use "Dental" GAND global classification as we describe
 861 tooth by tooth along the dental arch from right to left (Table 1) [17]. The dental
 862 classification by Bezerra et al., is only limited to the central and lateral incisors
 863 (Table 1) [67]. We describe also the 3D position of all of the teeth on the dental arch
 864 starting from posterior to anterior, and using the six degree of freedom reference
 865 frame (3 translations and 3 rotations) [56]. As Santos et al., we systematically
 866 describe the upper cervical spine [66], the atlas and the axis vertebra [58]. We are
 867 also using the natural contrast between the air and external soft tissue to evaluate the
 868 modifications in the shape of external ears that may occur in CLP syndromic
 869 patients. Moreover, we suggest the type of image modality such as axial, coronal,
 870 sagittal 2D view or 3D reconstruction which may be suited for a specific purpose.
 871 We provide with 46 freely accessible figures in contrast with only 3 available
 872 open-access figures from literature [67].
 873
 874

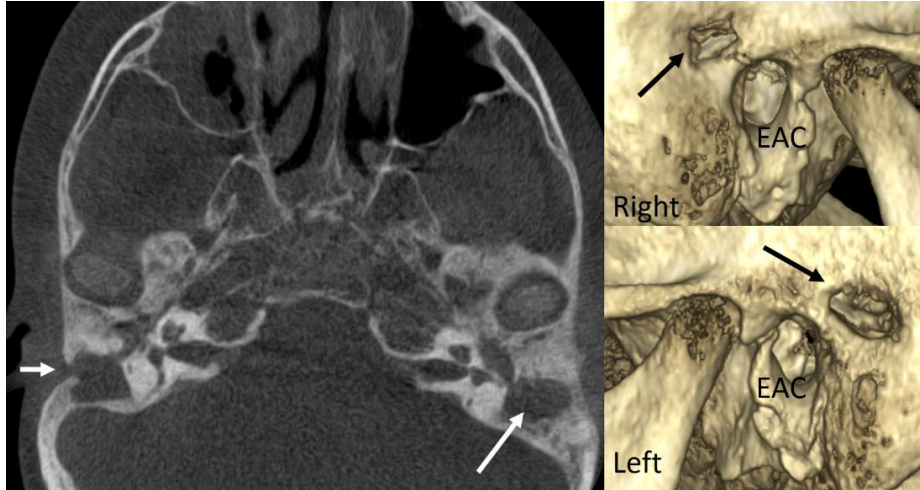
Table 1. Modes of reporting information from CBCT volume.

Modes of reporting	Literature methodologies	Our methodology
General approach		
Miles et al (2014) [64]	1) Paranasal sinuses, 2) Nasal cavity, 3) Airway, 4) Cervical structures, 5) TMJs, 6) Dental findings, 7) Other findings	Include: Paranasal sinuses, nasal cavity, cervical structures, dental findings Exclude: airway, TMJ
Kachlan et al (2021) [65]	1) Jaws, 2) Paranasal sinus, 3) Nasal fossa, 4) Pharyngeal airway, 5) Neck soft tissues, 6) TMJ, 7) Skull base/brain, and 8) Others	
Cleft palate general description		
Santos et al (2020) [66]	1) Paranasal sinuses, 2) Pharynx (airway), 3) Cervical spine, 4) TMJ, 5) Maxilla, and 6) Mandible, and 7) Abnormal teeth*, 8) Orbit, 9) Middle and inner ear cavity,	Include: paranasal sinuses, cervical spine, maxilla, skull Exclude: airway, mandible, orbit, middle and inner ear cavity

	10) Skull	*Not limited to the description of only abnormal teeth
Barbosa et al (2016) [17] GAND classification		
	Gap: notch, small, large size of the gap	Not used
	Arch: aligned, anterior constriction, anterior and posterior constriction	Not used
	Nasal: nasal floor: (cleft palate): notch, small, large	More descriptive approach (complete, partial cleft palate, anterior, posterior, fistula)
	Dental: normal, supernumerary/malformed, missing	Full description of all maxillary teeth
Bezerra et al (2017) [67] Tooth development in CLP patients		
	Agenesis (second incisor, second premolar)	Not limited to this category only
	Microdontia (conical lateral incisor)	Not limited to this category only
	Giroversion (central incisor)	Not limited to this category only

875
876
877
878
879
880
881
882
883
884
885
886
887
888
889
890
891
892
893

We are using large field of view (16x6.2cm) which may contain temporal bone. The international recommendations from 2011 insist on the dentist responsibility of reporting on the entire field of view [63]. Therefore, future development of our methodology should contain the systematic exploration of the middle and inner ear cavity (Figure 46) [66].



894

895 **Fig. 46. Planmeca Promax 3D Mid.** Patient 10 years-old. Axial view.
896 Arrows: traces of temporal bone surgery. 3D reconstruction. Right view:
897 arrow: surgical perforation of the right temporal bone in posterior and apical
898 to the right external auditory canal (EAC). Left side: arrow: surgical
899 perforation of the left temporal bone in apical to the left external auditory
900 canal.

901

902

- 903 • **Acknowledgements:** this study was presented at the Charity MedCongress for
 904 Ukraine army veterans, Lviv, Ukraine, 3.12.2022.
- 905 • **Funding sources statement:** this study does not receive any funding
- 906 • **Competing interests:** Prof R. Olszewski is Editor-in-Chief of Nemesis. The
 907 other authors declare no conflict of interest.
- 908 • **Ethical approval:** We obtained the approval from our University and Hospital
 909 Ethical committee for this study (B403/2019/03DEC/542)
- 910 • **Informed consent:** Patients were exempted from the informed consent
 911 according to the ethical committee approval.

912

Authors contribution:

Author	Contributor role
Olszewski Raphael	Conceptualization, Investigation, Methodology, Data curation, Resources, Validation, Writing original draft preparation, Supervision, Writing review and editing
De Muylder Antoine	Data curation, Writing review and editing
Siciliano Sergio	Data curation, Writing review and editing

913

914

915

References

916

917

918

919

920

921

1. Gümrü B, Guldali M, Tarcin B, Idman E, Sertac Peker M. Evaluation of cone beam computed tomography referral profile: Retrospective study in a Turkish paediatric subpopulation. Eur J Paediatr Dent 2021;22:66-70. <https://doi.org/10.23804/ejpd.2021.22.01.12>.

- 922 2. Theys S, Olszewski R. Cone beam computed tomography (CBCT) in pediatric
923 dentistry. *Nemesis* 2022;25:1-43. <https://doi.org/10.14428/nemesis.v25i1>.
924
- 925 3. Kuijpers MA, Chiu YT, Nada RM, Carels CE, Fudalej PS. Three-dimensional
926 imaging methods for quantitative analysis of facial soft tissues and skeletal
927 morphology in patients with orofacial clefts: a systematic review. *PLoS One*
928 2014;9:e93442. <https://doi.org/10.1371/journal.pone.0093442>.
929
- 930 4. Kuijpers-Jagtman AM, Kuijpers MAR, Schols GJH, Maal TJJ, Breuning KH, van
931 Vlijmen OJC. The use of cone-beam computed tomography for orthodontic
932 purposes. *Seminars Orthod* 2013;19:196-203.
933
- 934 5. Coşkun İ, Kaya B. Cone beam computed tomography in orthodontics. *Turk J*
935 *Orthod* 2018;31: 55–61. <https://doi.org/10.5152/TurkJOrthod.2018.18020>.
936
- 937 6. De Grauwe A, Ayaz I, Shujaat S, Dimitrov S, Gbadegbegnon L, Vande Vannet B,
938 Jacobs R. CBCT in orthodontics: a systematic review on justification of CBCT in a
939 paediatric population prior to orthodontic treatment. *Eur J Orthod* 2019;41:381-389.
940 <https://doi.org/10.1093/ejo/cjy066>.
941
- 942 7. Kapila SD, Nervina JM. CBCT in orthodontics: assessment of treatment outcomes
943 and indications for its use. *Dentomaxillofac Radiol* 2015;44:20140282.
944 <https://doi.org/10.1259/dmfr.20140282>.
945
- 946 8. Etemadi Sh M, Movahedian Attar B, Mehdizadeh M, Tajmiri G. Evaluation of the
947 CBCT imaging accuracy in the volumetric assessment of unilateral alveolar cleft. *J*
948 *Stomatol Oral Maxillofac Surg* 2021;122:e1-e5.
949 <https://doi.org/10.1016/j.jormas.2021.06.006>.
950
- 951 9. Janssen NG, Schreurs R, Bittermann GKP, Borstlap WA, Koole R, Meijer GJ,
952 Maal TJJ. A novel semi-automatic segmentation protocol for volumetric assessment
953 of alveolar cleft grafting procedures. *J Craniomaxillofac Surg* 2017;45:685-689.
954 <https://doi.org/10.1016/j.jcms.2017.02.018>.
955
- 956 10. Zhou WN, Xu YB, Jiang HB, Wan L, Du YF. Accurate evaluation of cone-beam
957 computed tomography to volumetrically assess bone grafting in alveolar cleft
958 patients. *J Craniofac Surg* 2015;26:e535-e539.
959 <https://doi.org/10.1097/SCS.0000000000002034>.
960
- 961 11. Dissaux C, Bodin F, Grollemund B, Bridonneau T, Kauffmann I, Mattern JF,
962 Bruant-Rodier C. Evaluation of success of alveolar cleft bone graft performed at 5
963 years versus 10 years of age. *J Craniomaxillofac Surg* 2016;44:21-26.
964 <https://doi.org/10.1016/j.jcms.2015.09.003>.
965

- 966 12. Chen PR, Lin YC, Pai BC, Tseng HJ, Lo LJ, Chou PY. Progressive comparison
967 of density assessment of alveolar bone graft in patients with unilateral and bilateral
968 cleft. *J Clin Med* 2021;10:5143. <https://doi.org/10.3390/jcm10215143>.
969
- 970 13. Linderup BW, Cattaneo PM, Jensen J, K seler A. Mandibular symphyseal bone
971 graft for reconstruction of alveolar cleft defects: Volumetric assessment with cone
972 beam computed tomography 1-year postsurgery. *Cleft Palate Craniofac J*
973 2016;53:64-72. <https://doi.org/10.1597/14-143>.
974
- 975 14. Kochhar AS, Sidhu MS, Prabhakar M, Bhasin R, Kochhar GK, Dadlani H,
976 Spagnuolo G, Mehta VV. Intra- and interobserver reliability of bone volume
977 estimation using OsiriX software in patients with cleft lip and palate using cone
978 beam computed tomography. *Dent J (Basel)* 2021;9:14.
979 <https://doi.org/10.3390/dj9020014>.
980
- 981 15. Datana S, Chattopadhyay PK, Kadu A. Bony bridge resorption after secondary
982 alveolar grafting and correlation with success of orthodontic treatment: A
983 prospective volumetric cone beam computed tomography (CBCT) study. *Med J*
984 *Armed Forces India* 2019;75:375-382. <https://doi.org/10.1016/j.mjafi.2018.02.005>.
985
- 986 16. Suomalainen A,  berg T, Rautio J, Hurmerinta K. Cone beam computed
987 tomography in the assessment of alveolar bone grafting in children with unilateral
988 cleft lip and palate. *Eur J Orthod* 2014;36:603-611.
989 <https://doi.org/10.1093/ejo/cjt105>.
990
- 991 17. Barbosa GL, Emodi O, Pretti H, van Aalst JA, de Almeida SM, Tyndall DA,
992 Pimenta LA. GAND classification and volumetric assessment of unilateral cleft lip
993 and palate malformations using cone beam computed tomography. *Int J Oral*
994 *Maxillofac Surg* 2016;45:1333-1340. <https://doi.org/10.1016/j.ijom.2016.05.008>.
995
- 996 18. Attar BM, Soltani P, Davari D, Mehdizadeh M. Cone-beam computed
997 tomographic comparison of chin symphysis bone particles and allograft versus iliac
998 crest bone graft alone for reconstruction of alveolar bone defects in cleft patients. *J*
999 *Korean Assoc Oral Maxillofac Surg* 2022;48:85-93.
1000 <https://doi.org/10.5125/jkaoms.2022.48.2.85>.
1001
- 1002 19. Padwa BL, Tio P, Garkhail P, Nuzzi LC. Cone beam computed tomographic
1003 analysis demonstrates a 94% radiographic success rate in 783 alveolar bone grafts. *J*
1004 *Oral Maxillofac Surg* 2022;80:633-640. <https://doi.org/10.1016/j.joms.2021.12.004>.
1005
- 1006 20. Gu Y, Yan C, Yan Z, Wang X, Yue L, Li L. Evaluation of the clinical efficacy
1007 and safety of modified alveolar cleft bone graft with cone-beam CT digital imaging
1008 in children. *Transl Pediatr* 2022;11:1140-1148. <https://doi.org/10.21037/tp-22-214>.
1009

- 1010 21. Oberoi S, Gill P, Chigurupati R, Hoffman WY, Hatcher DC, Vargervik K.
1011 Three-dimensional assessment of the eruption path of the canine in individuals with
1012 bone-grafted alveolar clefts using cone beam computed tomography. *Cleft Palate*
1013 *Craniofac J* 2010;47:507-512. <https://doi.org/10.1597/08-171>.
1014
- 1015 22. Touzet-Roumazeille S, Vi-Fane B, Kadlub N, Genin M, Dissaux C, Raoul G,
1016 Ferri J, Vazquez MP, Picard A. Osseous and dental outcomes of primary
1017 gingivoperiosteoplasty with iliac bone graft: A radiological evaluation. *J Cranio-*
1018 *maxillofac Surg* 2015;43:950-955. <https://doi.org/10.1016/j.jcms.2015.03.027>.
1019
- 1020 23. Linderup BW, K seler A, Jensen J, Cattaneo PM. A novel semiautomatic
1021 technique for volumetric assessment of the alveolar bone defect using cone beam
1022 computed tomography. *Cleft Palate Craniofac J* 2015;52:e47-55.
1023 <https://doi.org/10.1597/13-287>.
1024
- 1025 24. Garib DG, Yatabe MS, Ozawa TO, Filho OG. Alveolar bone morphology in
1026 patients with bilateral complete cleft lip and palate in the mixed dentition: cone
1027 beam computed tomography evaluation. *Cleft Palate Craniofac J* 2012;49:208-214.
1028 <https://doi.org/10.1597/10-198>.
1029
- 1030 25. Girinon F, Ketoff S, Hennocq Q, Kogane N, Ullman N, Kadlub N, Galliani E,
1031 Neiva-Vaz C, Vazquez MP, Picard A, Khonsari RH. Maxillary shape after primary
1032 cleft closure and before alveolar bone graft in two different management protocols:
1033 A comparative morphometric study. *J Stomatol Oral Maxillofac Surg* 2019;120:406-
1034 409. <https://doi.org/10.1016/j.jormas.2019.02.001>.
1035
- 1036 26. Hechler SL. Cone-beam CT: applications in orthodontics. *Dent Clin North Am*
1037 2008;52:809-823. <https://doi.org/10.1016/j.cden.2008.05.001>.
1038
- 1039 27. Tadinada A, Schneider S, Yadav S. Role of cone beam computed tomography in
1040 contemporary orthodontics. *Semin Orthod* 2018;24:407-415.
1041 <https://doi.org/10.1053/j.sodo.2018.10.005>.
1042
- 1043 28. Nervina JM. Cone beam computed tomography use in orthodontics. *Austral*
1044 *Dent J* 2012;57:95-102. <https://doi.org/10.1111/j.1834-7819.2011.01662.x>.
1045
- 1046 29. Parveen S, Husain A, Mascarenhas R, Reddy SG. Clinical utility of cone-beam
1047 computed tomography in patients with cleft lip palate: Current perspectives and
1048 guidelines. *J Cleft Lip Palate Craniofac Anomal* 2018;5:74-87.
1049 https://doi.org/10.4103/jclpca.jclpca_7_18.
1050
- 1051 30. Singh S, Batra P, Raghavan S, Sharma K, Srivastava A. Evaluation of Alt-
1052 RAMEC with facemask in patients with unilateral cleft lip and palate (UCLP) using
1053 cone beam computed tomography (CBCT) and finite element modeling-A clinical

- 1054 prospective study. *Cleft Palate Craniofac J.* 2022;59:166-176.
1055 <https://doi.org/10.1177/10556656211000968>.
- 1056
- 1057 31. de Almeida AM, Ozawa TO, Alves ACM, Janson G, Lauris JRP, Ioshida MSY,
1058 Garib DG. Slow versus rapid maxillary expansion in bilateral cleft lip and palate: a
1059 CBCT randomized clinical trial. *Clin Oral Investig* 2017;21:1789-1799.
1060 <https://doi.org/10.1007/s00784-016-1943-8>.
- 1061
- 1062 32. Steegman RM, Klein Meulekamp AF, Dieters A, Jansma J, van der Meer WJ,
1063 Ren Y. Skeletal changes in growing cleft patients with class III malocclusion treated
1064 with bone anchored maxillary protraction-A 3.5-year follow-up. *J Clin Med*
1065 2021;10:750. <https://doi.org/10.3390/jcm10040750>.
- 1066
- 1067 33. Ren Y, Steegman R, Dieters A, Jansma J, Stamatakis H. Bone-anchored maxil-
1068 lary protraction in patients with unilateral complete cleft lip and palate and Class III
1069 malocclusion. *Clin Oral Investig* 2019;23:2429-2441.
1070 <https://doi.org/10.1007/s00784-018-2627-3>.
- 1071
- 1072 34. Alrejaye N, Gao J, Hatcher D, Oberoi S. Effect of maxillary expansion and
1073 protraction on the oropharyngeal airway in individuals with non-syndromic cleft
1074 palate with or without cleft lip. *PLoS One* 2019;14:e0213328.
1075 <https://doi.org/10.1371/journal.pone.0213328>.
- 1076
- 1077 35. Stangherlin Gomes O, Carvalho RM, Faco R, Yatabe M, Ozawa TO, De Clerck
1078 H, Timmerman H, Garib D. Influence of bone-anchored maxillary protraction on
1079 secondary alveolar bone graft status in unilateral complete cleft lip and palate. *Am J*
1080 *Orthod Dentofacial Orthop* 2020;158:731-737.
1081 <https://doi.org/10.1016/j.ajodo.2019.10.021>.
- 1082
- 1083 36. Garib D, Miranda F, Sathler R, Kuijpers-Jagtman AM, Aiello CA. Rapid maxil-
1084 lary expansion after alveolar bone grafting with rhBMP-2 in UCLP evaluated by
1085 means of CBCT. *Cleft Palate Craniofac J* 2017;54:474-480.
1086 <https://doi.org/10.1597/15-133>.
- 1087
- 1088 37. Parveen S, Husain A, Johns G, Mascarenhas R, Reddy SG. Three-dimensional
1089 analysis of craniofacial structures of individuals with nonsyndromic unilateral
1090 complete cleft lip and palate. *J Craniofac Surg* 2021;32:e65-e69.
1091 <https://doi.org/10.1097/SCS.0000000000006933>.
- 1092
- 1093 38. Yang L, Chen Z, Zhang X. A cone-beam computed tomography evaluation of
1094 facial asymmetry in unilateral cleft lip and palate individuals. *J Oral Sci*
1095 2016;58:109-115. <https://doi.org/10.2334/josnurd.58.109>.
- 1096
- 1097 39. Lin Y, Chen G, Fu Z, Ma L, Li W. Cone-beam computed tomography assess-
1098 ment of lower facial asymmetry in unilateral cleft lip and palate and non-cleft

- 1099 patients with class III skeletal relationship. *PLoS One* 2015;10:e0130235.
 1100 <https://doi.org/10.1371/journal.pone.0130235>.
 1101
- 1102 40. Shrestha A, Takahashi M, Yamaguchi T, Adel M, Furuhashi M, Hikita Y,
 1103 Yoshida H, Nakawaki T, Maki K. Three-dimensional evaluation of mandibular
 1104 volume in patients with cleft lip and palate during the deciduous dentition period.
 1105 *Angle Orthod* 2020;90:85-91. <https://doi.org/10.2319/112618-831.1>.
 1106
- 1107 41. Yatabe M, Garib D, Faco R, de Clerck H, Souki B, Janson G, Nguyen T,
 1108 Cevidane L, Ruellas A. Mandibular and glenoid fossa changes after bone-anchored
 1109 maxillary protraction therapy in patients with UCLP: A 3-D preliminary assessment.
 1110 *Angle Orthod* 2017;87:423-431. <https://doi.org/10.2319/052516-419.1>.
 1111
- 1112 42. Akay G, Eren I, Karadag O, Gungor K. Three-dimensional assessment of the
 1113 sella turcica: comparison between cleft lip and palate patients and skeletal
 1114 malocclusion classes. *Surg Radiol Anat* 2020;42:977-983.
 1115 <https://doi.org/10.1007/s00276-020-02481-z>.
 1116
- 1117 43. Kiaee B, Nucci L, Sarkarat F, Talaeipour AR, Eslami S, Amiri F, Jamilian A.
 1118 Three-dimensional assessment of airway volumes in patients with unilateral cleft lip
 1119 and palate. *Prog Orthod*. 2021;22:35. <https://doi.org/10.1186/s40510-021-00382-4>.
 1120
- 1121 44. Pimenta LA, de Rezende Barbosa GL, Pretti H, Emodi O, van Aalst J, Rossouw
 1122 PE, Tyndall DA, Drake AF. Three-dimensional evaluation of nasopharyngeal
 1123 airways of unilateral cleft lip and palate patients. *Laryngoscope* 2015;125:736-739.
 1124 <https://doi.org/10.1002/lary.24895>.
 1125
- 1126 45. Cheung T, Oberoi S. Three dimensional assessment of the pharyngeal airway in
 1127 individuals with non-syndromic cleft lip and palate. *PLoS One* 2012;7:e43405.
 1128 <https://doi.org/10.1371/journal.pone.0043405>.
 1129
- 1130 46. Takahashi M, Yamaguchi T, Lee MK, Suzuki Y, Adel M, Tomita D, Nakawaki
 1131 T, Yoshida H, Hikita Y, Furuhashi M, Tsuneoka M, Nagahama R, Marazita ML,
 1132 Weinberg SM, Maki K. Three-dimensional assessment of the pharyngeal airway in
 1133 Japanese preschoolers with orofacial clefts. *Laryngoscope* 2020;130:533-540.
 1134 <https://doi.org/10.1002/lary.27957>.
 1135
- 1136 47. Iwasaki T, Suga H, Minami-Yanagisawa A, Hashiguchi-Sato M, Sato H,
 1137 Yamamoto Y, Shirazawa Y, Tsujii T, Kanomi R, Yamasaki Y. Upper airway in
 1138 children with unilateral cleft lip and palate evaluated with computational fluid
 1139 dynamics. *Am J Orthod Dentofacial Orthop* 2019;156:257-265.
 1140 <https://doi.org/10.1016/j.ajodo.2018.09.013>.
 1141
- 1142 48. Al-Fahdawi MA, El-Kassaby MA, Farid MM, El-Fotouh MA. Cone beam com-
 1143 puted tomography analysis of oropharyngeal airway in preadolescent nonsyndromic

- 1144 bilateral and unilateral cleft lip and palate patients. *Cleft Palate Craniofac J*
1145 2018;55:883-890. <https://doi.org/10.1597/15-322>.
1146
- 1147 49. Ko J, Han HJ, Hoffman W, Oberoi S. Three-dimensional analysis of cortical
1148 bone thickness in individuals with non-syndromic unilateral cleft lip and palate. *J*
1149 *Craniofac Surg* 2019;30:2094-2098.
1150 <https://doi.org/10.1097/SCS.0000000000005988>.
1151
- 1152 50. Moscarino S, Scholz J, Bastian A, Knaup I, Wolf M. Bone and soft tissue palatal
1153 morphology and potential anchorage sides in cleft palate patients. *Ann Anat*
1154 2019;224:41-46. <https://doi.org/10.1016/j.aanat.2019.02.005>.
- 1155 51. Kang BC, Yoon SJ, Lee JS, Al-Rawi W, Palomo JM. The use of cone beam
1156 computed tomography for the evaluation of pathology, developmental anomalies
1157 and traumatic injuries relevant to orthodontics. *Semin Orthod* 2011;17:20-33.
1158 <https://doi.org/10.1053/j.sodo.2010.08.005>.
- 1159 52. Lopes de Rezende Barbosa G, Pimenta LA, Pretti H, Golden BA, Roberts J,
1160 Drake AF. Difference in maxillary sinus volumes of patients with cleft lip and
1161 palate. *Int J Pediatr Otorhinolaryngol* 2014;78:2234-2236.
1162 <https://doi.org/10.1016/j.ijporl.2014.10.019>.
1163
- 1164 53. Wang X, Zhang M, Han J, Wang H, Li S. Three-dimensional evaluation of
1165 maxillary sinus and maxilla for adolescent patients with unilateral cleft lip and
1166 palate using cone-beam computed tomography. *Int J Pediatr Otorhinolaryngol*
1167 2020;135:110085. <https://doi.org/10.1016/j.ijporl.2020.110085>.
1168
- 1169 54. Li J, Shi B, Liu K, Zheng Q. A preliminary study on the hard-soft tissue
1170 relationships among unoperated secondary unilateral cleft nose deformities. *Oral*
1171 *Surg Oral Med Oral Pathol Oral Radiol* 2012;113:300-307.
1172 <https://doi.org/10.1016/j.tripleo.2011.03.007>.
1173
- 1174 55. Massie JP, Bruckman K, Rifkin WJ, Runyan CM, Shetye PR, Grayson B, Flores
1175 RL. The effect of nasoalveolar molding on nasal airway anatomy: A 9-year follow-
1176 up of patients with unilateral cleft lip and palate. *Cleft Palate Craniofac J*
1177 2018;55:596-601. <https://doi.org/10.1177/1055665617744062>.
1178
- 1179 56. Alqahtani K, Shaheen E, Shujaat S, EzEldeen M, Dormaar T, de Llano-Pérua
1180 MC, Politis C, Jacobs R. Validation of a novel method for canine eruption
1181 assessment in unilateral cleft lip and palate patients. *Clin Exp Dent Res* 2021;7:285-
1182 292. <https://doi.org/10.1002/cre2.397>.
1183
- 1184 57. Sandhu SK. Cone beam computed tomography in orthodontics. *Saint's Int Dent J*
1185 2017;3:1-3. https://doi.org/10.4103/sidj.sidj_1_18.

- 1186
1187
1188
1189
1190
1191
1192
1193
1194
1195
1196
1197
1198
1199
1200
1201
1202
1203
1204
1205
1206
1207
1208
1209
1210
1211
1212
1213
1214
1215
1216
1217
1218
1219
1220
1221
1222
1223
1224
1225
1226
1227
1228
1229
58. Berrocal C, Terrero-Pérez A, Peralta-Mamani M, Fischer Rubira-Bullen IR, Marques Honorio H, Marchi de Carvalho IM, Alvares Capelozza AL. Cervical vertebrae anomalies and cleft lip and palate: a systematic review and meta-analysis. *Dentomaxillofac Radiol* 2019;48: 20190085. <https://doi.org/10.1259/dmfr.20190085>.
59. Patel S, Harvey S. Guidelines for reporting on CBCT scans. *Int Endod J* 2021;54:628-633. <https://doi.org/10.1111/iej.13443>.
60. Kim IH, Singer SR, Mupparapu M. Review of cone beam computed tomography guidelines in North America. *Quintessence Int* 2019;50:136-145. <https://doi.org/10.3290/j.qia.41332>.
61. Harvey S, Patel S. Guidelines and template for reporting on CBCT scans. *Br Dent J* 2020;228:15-18. <https://doi.org/10.1038/s41415-019-1115-8>.
62. Noar JH, Pabari S. Cone beam computed tomography--current understanding and evidence for its orthodontic applications? *J Orthod* 2013;40:5-13. <https://doi.org/10.1179/1465313312Y.0000000040>.
63. Scarfe WC, Li Z, Aboelmaaty W, Scott SA, Farman AG. Maxillofacial cone beam computed tomography: essence, elements and steps to interpretation. *Aust Dent J* 2012;57:46-60. <https://doi.org/10.1111/j.1834-7819.2011.01657.x>.
64. Miles DA, Danforth RA. Reporting findings in the cone beam computed tomography volume. *Dent Clin North Am* 2014;58:687-709. <https://doi.org/10.1016/j.cden.2014.04.006>.
65. Kachlan MO, Yang J, Balshi TJ, Wolfinger GJ, Balshi SF. Incidental findings in cone beam computed tomography for dental implants in 1002 patients. *J Prosthodont* 2021;30:665-675. <https://doi.org/10.1111/jopr.13329>.
66. Santos G, Ickow I, Job J, Brooker JE, Dvoracek LA, Rigby E, Shah N, Chen W, Branstetter B, Schuster LA. Cone-beam computed tomography incidental findings in individuals with cleft lip and palate. *Cleft Palate Craniofac J* 2020;57:404-411. <https://doi.org/10.1177/1055665619897469>.
67. Bezerra BT, Pinho JN, da Silva LC. Tooth abnormalities in individuals with unilateral alveolar clefts: A comparison between sides using cone-beam computed tomography. *J Clin Exp Dent* 2017;9:e1195-e1200. <https://doi.org/10.4317/jced.54043>.